



AN 32-ER  
218050

TARGET SIGNATURE MODELING AND  
BISTATIC SCATTERING MEASUREMENT STUDIES

W. D. Burnside, T. H. Lee, R. Rojas  
R. J. Marhefka, D. Bensman

The Ohio State University  
**ElectroScience Laboratory**

Department of Electrical Engineering  
Columbus, Ohio 43212

Semi-Annual Report  
721432-1, 721446-1, 721447-1, and 721711-1  
Grant No. NAG2-542  
September 1988 - February 1989

NASA - Ames Research Center  
Moffett Field, CA 94035

(NASA-CR-185434) TARGET SIGNATURE MODELING  
AND BISTATIC SCATTERING MEASUREMENT STUDIES  
Semiannual Report, Sep. 1988 - Feb. 1989  
{Ohio State Univ.} 56 p CSCL 17I

N89-27870

Unclas  
G3/32 0218050

## NOTICES

When Government drawings, specifications, or other data are used for any purpose other than in connection with a definitely related Government procurement operation, the United States Government thereby incurs no responsibility nor any obligation whatsoever, and the fact that the Government may have formulated, furnished, or in any way supplied the said drawings, specifications, or other data, is not to be regarded by implication or otherwise as in any manner licensing the holder or any other person or corporation, or conveying any rights or permission to manufacture, use, or sell any patented invention that may in any way be related thereto.

<b>REPORT DOCUMENTATION PAGE</b>	<b>1. REPORT NO.</b>	<b>2.</b>	<b>3. Recipient's Accession No.</b>
<b>4. Title and Subtitle</b> Target Signature Modeling and Bistatic Scattering Measurement Studies			<b>5. Report Date</b> Sept. 1988 - Feb. 1989
<b>7. Author(s)</b> W.D. Burnside, T.H. Lee, R. Rojas R.J. Marhefka, D. Bensman			<b>6.</b>
<b>9. Performing Organization Name and Address</b> The Ohio State University ElectroScience Laboratory 1320 Kinnear Road Columbus, OH 43212			<b>8. Performing Org. Rept. No.</b> 721432-1, 721446-1, 721447-1, 721711-1
<b>12. Sponsoring Organization Name and Address</b> University Affairs Branch, NASA - Ames Research Center M/S 241-25 Moffett Field, CA 94035			<b>10. Project/Task/Work Unit No.</b>
<b>15. Supplementary Notes</b>			<b>11. Contract(C) or Grant(G) No.</b> (C) (G) NAG2-542
<b>16. Abstract (Limit: 200 words)</b>  This is a semi-annual report that summarized the work done on Grant No. NAG2-542 during the period 1 September 1988 to 28 February 1989. There are four areas of study to be summarized: 1) Bistatic scattering measurement studies for a compact range. 2) Target signature modeling for test and evaluation hardware in the loop situations. 3) Aircraft code modification study. 4) SATCOM antenna studies on aircraft.			<b>13. Report Type/Period Covered</b> Semi-Annual Report
<b>17. Document Analysis a. Descriptors</b>  <b>b. Identifiers/Open-Ended Terms</b>  <b>c. COSATI Field/Group</b>			<b>14.</b>
<b>18. Availability Statement</b> A. Approved for public release; Distribution is unlimited.		<b>19. Security Class (This Report)</b> Unclassified	<b>21. No. of Pages</b> 55
		<b>20. Security Class (This Page)</b> Unclassified	<b>22. Price</b>

**Blank Page**

# Contents

<b>List of Figures</b>	<b>v</b>
<b>1 Introduction</b>	<b>1</b>
<b>2 Bistatic Measurement Study</b>	<b>2</b>
2.1 Introduction . . . . .	2
2.2 Approach . . . . .	3
2.3 Results . . . . .	5
2.4 Summary and Conclusions . . . . .	18
2.5 Acknowledgement . . . . .	18
<b>3 Target Signature Study</b>	<b>19</b>
3.1 Introduction . . . . .	19
3.2 Scattering Code Overview . . . . .	19
3.3 Storage Requirements . . . . .	21
3.4 Further Work . . . . .	23
<b>4 Aircraft Code Study</b>	<b>24</b>
4.1 Introduction . . . . .	24
4.2 Smoothing Algorithm . . . . .	24
4.3 Patch Antenna . . . . .	25
4.4 PC Study . . . . .	25
<b>5 SATCOM Antenna Study</b>	<b>26</b>
5.1 Introduction . . . . .	26
5.2 Batwing Antenna . . . . .	26
5.3 Model Validation . . . . .	27
5.4 Further Work . . . . .	27



# List of Figures

2.1	Top view of bistatic scattering measurement in a compact range. (Transmit and receive compact ranges.) . . . . .	4
2.2	Top view of bistatic scattering measurement in a compact range. (Transmit compact range and receive horn antenna.) . . . . .	5
2.3	Bistatic scattering measurement of spheres in OSU compact range. . . . .	6
2.4	Positions of the 6" and 3.25" spheres for the bistatic scattering measurement. . . . .	8
2.5	Surface plot of the images for the 6" and 3.25" spheres obtained from the bistatic scattered fields. . . . .	9
2.6	Contour plot of the images for the 6" and 3.25" spheres obtained from the bistatic scattered fields. . . . .	10
2.7	Surface plot of the images for the 6" and 3.25" spheres obtained from the backscattered fields. . . . .	11
2.8	Contour plot of the images for the 6" and 3.25" spheres obtained from the backscattered fields. . . . .	12
2.9	Positions of the 6", 3.25" and 1" spheres for the bistatic scattering measurement. . . . .	13
2.10	Surface plot of the images for the 6", 3.25" and 1" spheres obtained from the bistatic scattered fields. . . . .	14
2.11	Contour plot of the images for the 6", 3.25" and 1" spheres obtained from the bistatic scattered fields. . . . .	15
2.12	Surface plot of the images for the 6", 3.25" and 1" spheres obtained from the backscattered fields. . . . .	16
2.13	Contour plot of the images for the 6", 3.25" and 1" spheres obtained from the backscattered fields. . . . .	17

5.1	Batwing airborne UHF satellite communication antenna of Dorne and Magolin. . . . .	28
5.2	Calculated Batwing right hand circular polarized antenna pattern at 244 MHz on an 8' ground plane using the NEC-BSC. . . . .	29
5.3	Measured Batwing right hand circular polarized antenna pattern at 244 MHz on an 8' ground plane. (Pattern supplied by Dorne and Margolin.) . . . . .	30
5.4	Calculated Batwing right hand circular polarized antenna pattern at 300 MHz on an infinite ground plane using the NEC-BSC. . . . .	31
5.5	Calculated Batwing right hand circular polarized antenna pattern at 300 MHz on an infinite ground plane using the ESP code. . . . .	32
5.6	Geometry of the model of the P3C aircraft code used in the NEC-BSC showing the location of the antenna. . . . .	33
5.7	UTD calculated roll plane pattern for batwing antenna on a P3C for right hand circular polarization in the roll plane at 300 MHz. . . . .	34
5.8	Boeing's measured roll plane pattern for batwing antenna on a P3C for right hand circular polarization in the roll plane at 300 MHz. . . . .	35
5.9	UTD calculated azimuth plane pattern for batwing antenna on a P3C for right hand circular polarization in the roll plane at 300 MHz. . . . .	36
5.10	Boeing's measured azimuth plane pattern for batwing antenna on a P3C for right hand circular polarization in the roll plane at 300 MHz. . . . .	37
5.11	UTD calculated elevation plane pattern for batwing antenna on a P3C for right hand circular polarization in the roll plane at 300 MHz. . . . .	38
5.12	Boeing's measured elevation plane pattern for batwing antenna on a P3C for right hand circular polarization in the roll plane at 300 MHz. . . . .	39
5.13	UTD calculated roll plane pattern for batwing antenna on a P3C for left hand circular polarization in the roll plane at 300 MHz. . . . .	40

5.14	Boeing's measured roll plane pattern for batwing antenna on a P3C for left hand circular polarization in the roll plane at 300 MHz. . . . .	41
5.15	UTD calculated azimuth plane pattern for batwing antenna on a P3C for left hand circular polarization in the roll plane at 300 MHz. . . . .	42
5.16	Boeing's measured azimuth plane pattern for batwing antenna on a P3C for left hand circular polarization in the roll plane at 300 MHz. . . . .	43
5.17	UTD calculated elevation plane pattern for batwing antenna on a P3C for left hand circular polarization in the roll plane at 300 MHz. . . . .	44
5.18	Boeing's measured elevation plane pattern for batwing antenna on a P3C for left hand circular polarization in the roll plane at 300 MHz. . . . .	45



# Chapter 1

## Introduction

This is an semi-annual report that summarizes the work done on Grant No. NAG2-542 during the period 1 September 1988 to 28 February 1989. There are four areas of study to be summarized:

1. Bistatic scattering measurement studies for a compact range. This work is being conducted by T. H. Lee and W. D. Burnside under Ohio State University project number 721432.
2. Target signature modeling for test and evaluation hardware in the loop situations. This work is being conducted by R. J. Marhefka under Ohio State University project number 721446.
3. Aircraft and missile code modification studies. This work is being conducted by R. Rojas under Ohio State University project number 721447.
4. SATCOM antenna studies on aircraft. This work is being conducted by R. J. Marhefka and D. Bensman under Ohio State University project number 721711.

An overview of the research accomplished is described in the separate chapters below.

# Chapter 2

## Bistatic Measurement Study

This is a brief review of the portion of the grant pertaining to bistatic measurement study over the period September 1, 1988 to February 28, 1989. The summary described here is to be presented at the AMTA meeting in August entitled "Imaging Processing of Bistatic Scattered Fields Obtained in a Compact Range," by T. H. Lee and W. D. Burnside.

### 2.1 Introduction

It is very important in diagnostic radar applications that one can accurately distinguish various dominant scattering terms associated with specific features on a target based on its scattering characteristics. Normally, the backscattered fields of the target are collected and processed to obtain the down-range and cross-range scattering centers [1]. The backscattered fields can be collected either in a far-field range or in a compact range. On the other hand, bistatic scattering of a target has been getting a lot of attention recently. Consequently, the determination of the dominant scattering centers using bistatic scattered fields of a target is also very important.

In this report, a general image processing technique which utilizes the bistatic scattered fields collected in a compact range is presented. The transmitting and receiving antennas can be either two compact

ranges or one compact range and a horn antenna. The compact range reflector can be either focussed or defocussed so that a near field situation can be simulated. The bistatic scattered fields are collected as a function of frequency and the angle of rotation of the target. Then, cross-range and down-range images of the target are determined. Experimental results are presented to validate this image processing technique.

## 2.2 Approach

Conventional image processing of backscattered fields for a target uses efficient algorithms such as a Fast Fourier Transform to determine the target image. This requires that the antenna be located a large distance from the target [2] and that the target be rotated only through small angles. However, these assumptions are not necessary in general. For example, it has been shown that one can use defocussed compact range system to simulate a near field illumination of the target [3]. In order to determine the image of the target from the collected backscattered fields, a more general image processing approach has to be implemented [2,3]. The key factor in general image processing is the knowledge of the phase history of the scattering center associated with a given illumination. The backscattered fields, which are normally collected as functions of frequency and target angular rotation, are processed by multiplying the received response by a phase factor which is the complex conjugate of the phase associated with the path length from the source of illumination to the potential scattering center and then to the receiver. This data is then summed to determine the image response. Using this approach, the response at a true scattering center is more enhanced than those which are not true scattering centers.

The same processing technique can be used to determine the scattering centers of a target from its bistatic scattered fields. Consider the bistatic scattering measurement configuration shown in Figures 2.1 and 2.2. The system can be either two compact ranges as shown in Figure 2.1 or one compact range and one horn antenna (or other an-

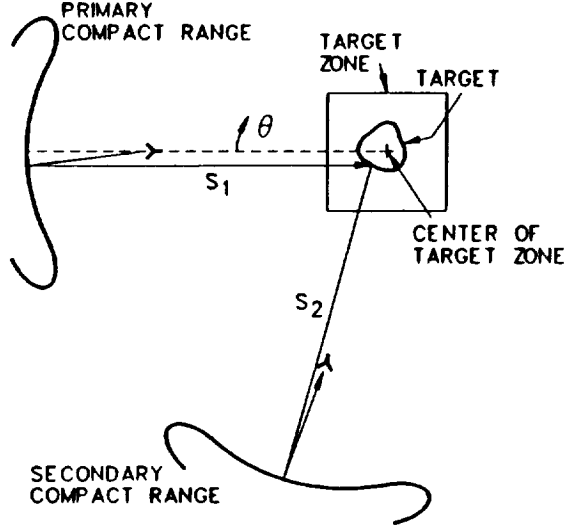


Figure 2.1: Top view of bistatic scattering measurement in a compact range. (Transmit and receive compact ranges.)

tennas) as shown in Figure 2.2. For a target located in the test zone, the bistatic scattered fields,  $E_s(f_m, \theta_n)$ , are collected for a series of frequencies,  $f_m$ , and a series of angles of rotation,  $\theta_n$ . The image of the target,  $I(\gamma_x, \gamma_z)$ , is determined by

$$I(\gamma_x, \gamma_z) = \sum_{m=1}^{m=M} \sum_{n=1}^{n=N} E_s(f_m, \theta_n) e^{j2\Phi(\gamma_x, \gamma_z, f_m, \theta_n)} \quad (2.1)$$

where

$$\Phi(\gamma_x, \gamma_z, f_m, \theta_n) = \frac{2\pi f_m}{c} (s_1 + s_2). \quad (2.2)$$

In Equations 2.1 and 2.2,  $s_1$  and  $s_2$  are the path lengths from the transmitting antenna to the point  $(\gamma_x, \gamma_z)$  on the image plane and from  $(\gamma_x, \gamma_z)$  to the receiving antenna,  $f_m$  is the  $m$ 'th frequency and  $\theta_n$  is the  $n$ 'th angle of rotation. It is apparent that if the point,  $(\gamma_x, \gamma_z)$ , is a scattering center, the bistatic scattered field,  $E_s$ , should have a phase factor,  $e^{-j2\Phi}$ , which is the complex conjugate of the phase factor shown in Equation 2.1. Consequently, the resulting image,  $I(\gamma_x, \gamma_z)$ , will peak up at the image location. On the other hand, if  $(\gamma_x, \gamma_z)$

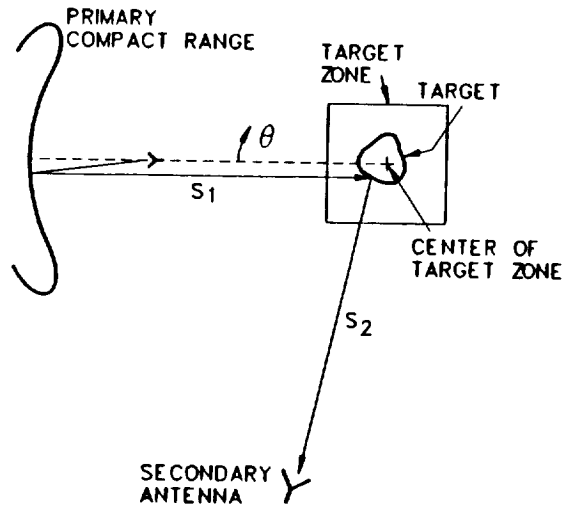


Figure 2.2: Top view of bistatic scattering measurement in a compact range. (Transmit compact range and receive horn antenna.)

is not a scattering center, the image will not be as significant. For each point on the image plane, one can determine the path lengths,  $s_1$  and  $s_2$ , and use Equation 2.1 to determine the complete image of the target. The frequency behaviour of the bistatic scattered fields provides the down range information; whereas, the angle responses provide the cross range location of the scattering centers.

Since the image processing method given by Equation 2.1 only requires the knowledge of the path lengths,  $s_1$  and  $s_2$ , the compact range reflector can be a defocused system so that one can simulate a near field situation. However, one has to determine the ray trajectory in order to find the point of reflection on the compact range reflector.

## 2.3 Results

A set of bistatic measurement has been performed at The Ohio State University ElectroScience Laboratory compact range facility. The configuration of the measurement is shown in Figure 2.3. Spheres

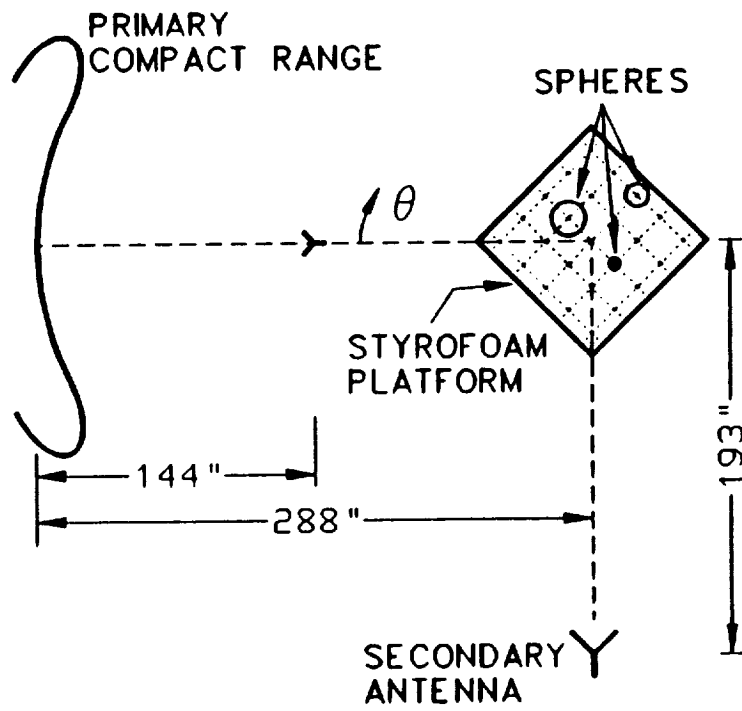


Figure 2.3: Bistatic scattering measurement of spheres in OSU compact range.

with diameters of 6", 3.25" and 1" were placed on a styrofoam platform which was then positioned at the center of the target zone. The compact range reflector has a focal distance of 12' and the center of the target zone is at 24' from the vertex of the reflector with a height of 60". The second antenna for the bistatic scattering measurement was located 193" from the center of the target zone in the direction perpendicular to the axis of the compact range reflector. The height of this antenna was the same as the center of the target zone. Several combinations of spheres were used as the target for these measurements. The target was rotated from  $-30^\circ$  to  $30^\circ$  with respect to the axis of the compact range reflector, and bistatic scattered fields were collected uniformly across the 2 to 18 GHz frequency band. Since the compact range has a capability of simultaneously collecting data from 2 different channels, the backscattered fields were also collected at the same time. Two image processing results based on these measurements are presented in this section.

The first combination of the spheres used as the target is shown in Figure 2.4. Note that a 6" sphere is located at X and a 3.25" sphere at N. The image of this target obtained by processing the bistatic scattered fields is shown in Figures 2.5 and 2.6. The backscattered fields can also be processed by using Equation 2.1 by simply assuming that the two compact range reflectors shown in Figure 2.1 are co-located. The resulting image is shown in Figures 2.7 and 2.8. From Figure 2.4, the center of the 6" sphere is at  $\gamma_x=8.485"$  and  $\gamma_z=0.0"$  and the center of the 3.25" sphere is at  $\gamma_x=-4.243"$  and  $\gamma_z=-12.728"$ . However, the scattering centers will not be at these locations because one has to take the radius of the spheres into account. The images shown in Figures 2.5 to 2.8 clearly indicate the scattering centers of this target. One also notices the movement of the sphere scattering centers from these images. This is because the target was rotated with respect to the center of the target zone which results in the movement of the scattering centers in that the sphere reflection point moves with the angles of incidence. In addition to these scattering centers, there are other peak responses that appear in these images. These are secondary scattering centers caused by the creeping waves associated with each sphere.

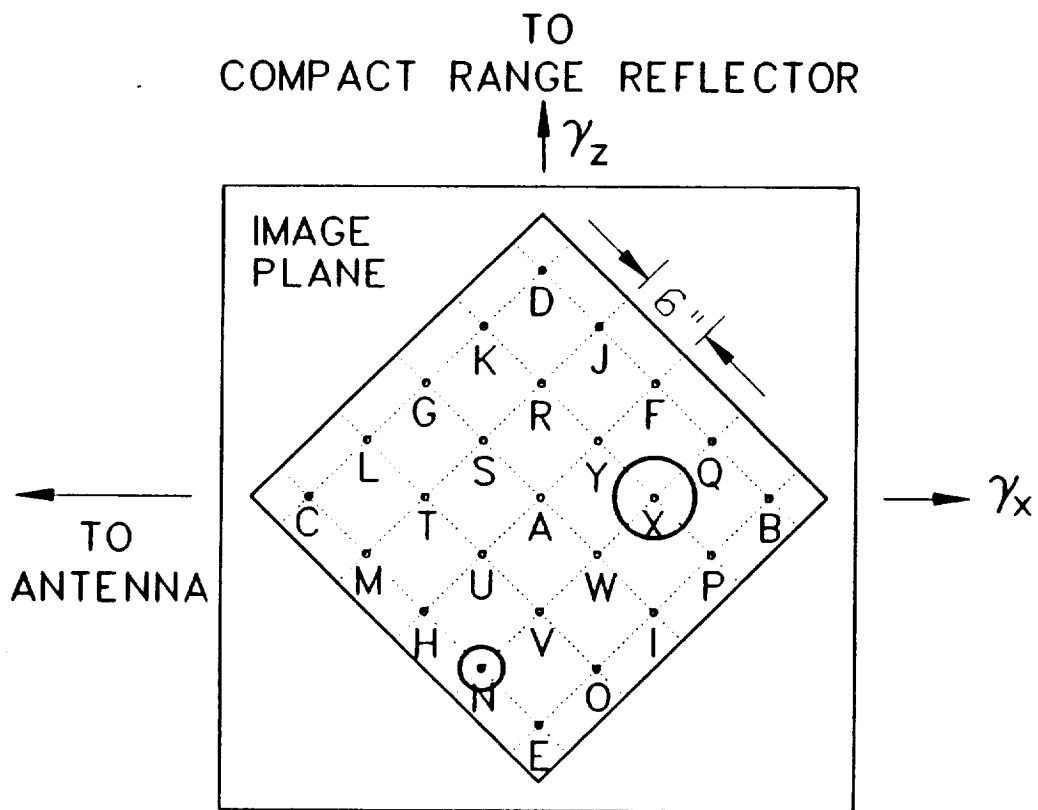


Figure 2.4: Positions of the 6" and 3.25" spheres for the bistatic scattering measurement.

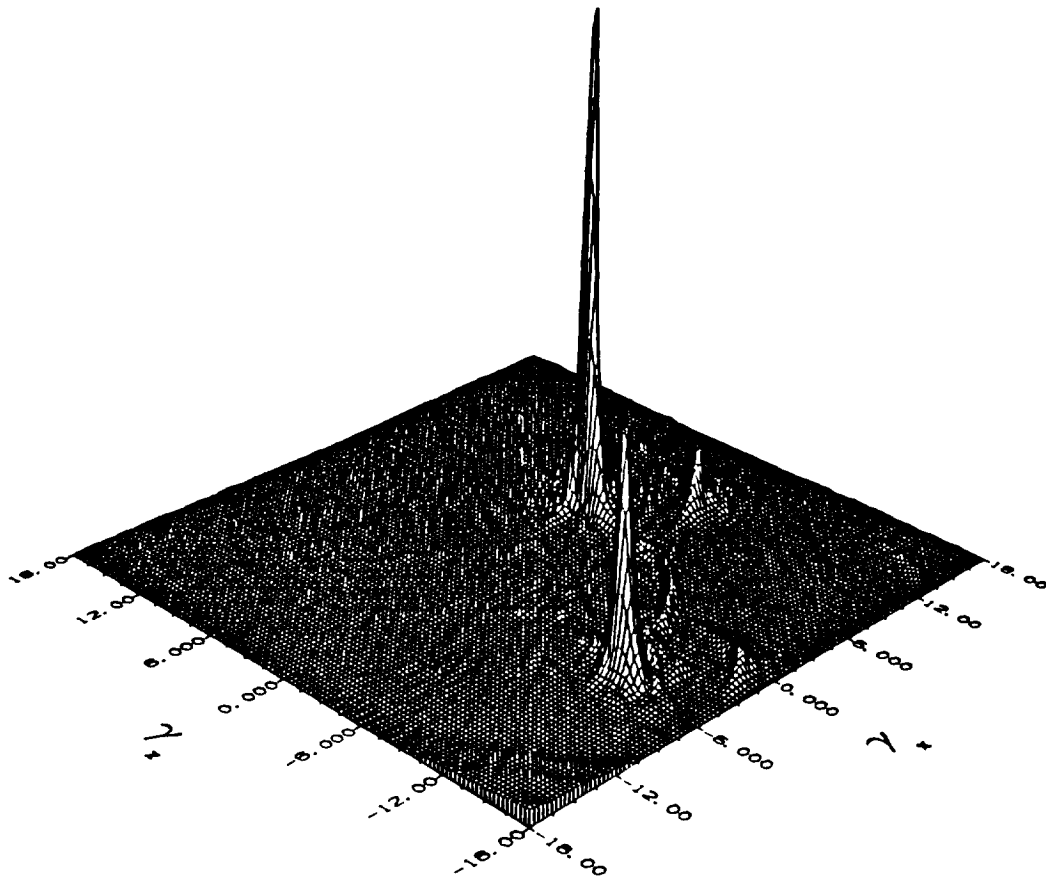


Figure 2.5: Surface plot of the images for the 6" and 3.25" spheres obtained from the bistatic scattered fields.

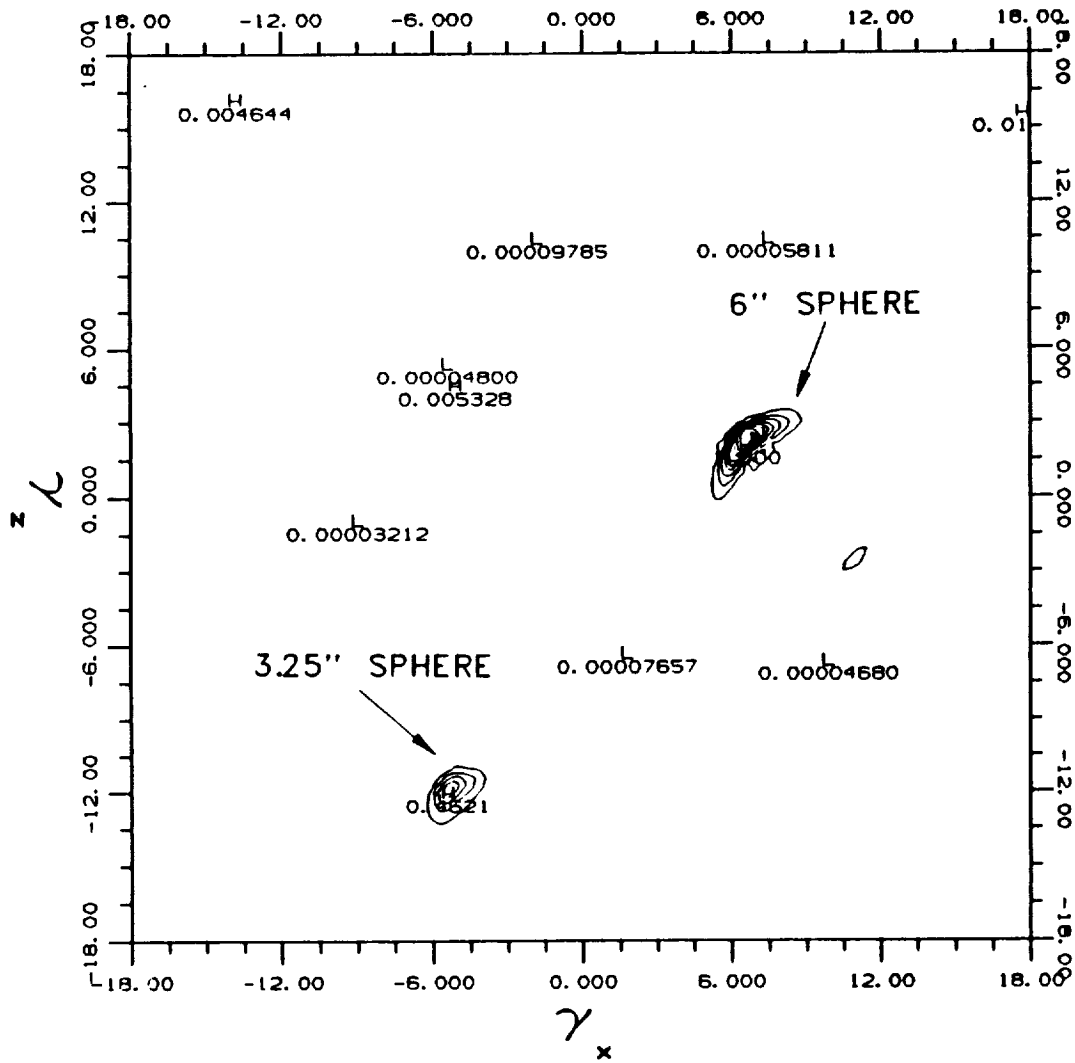


Figure 2.6: Contour plot of the images for the 6'' and 3.25'' spheres obtained from the bistatic scattered fields.

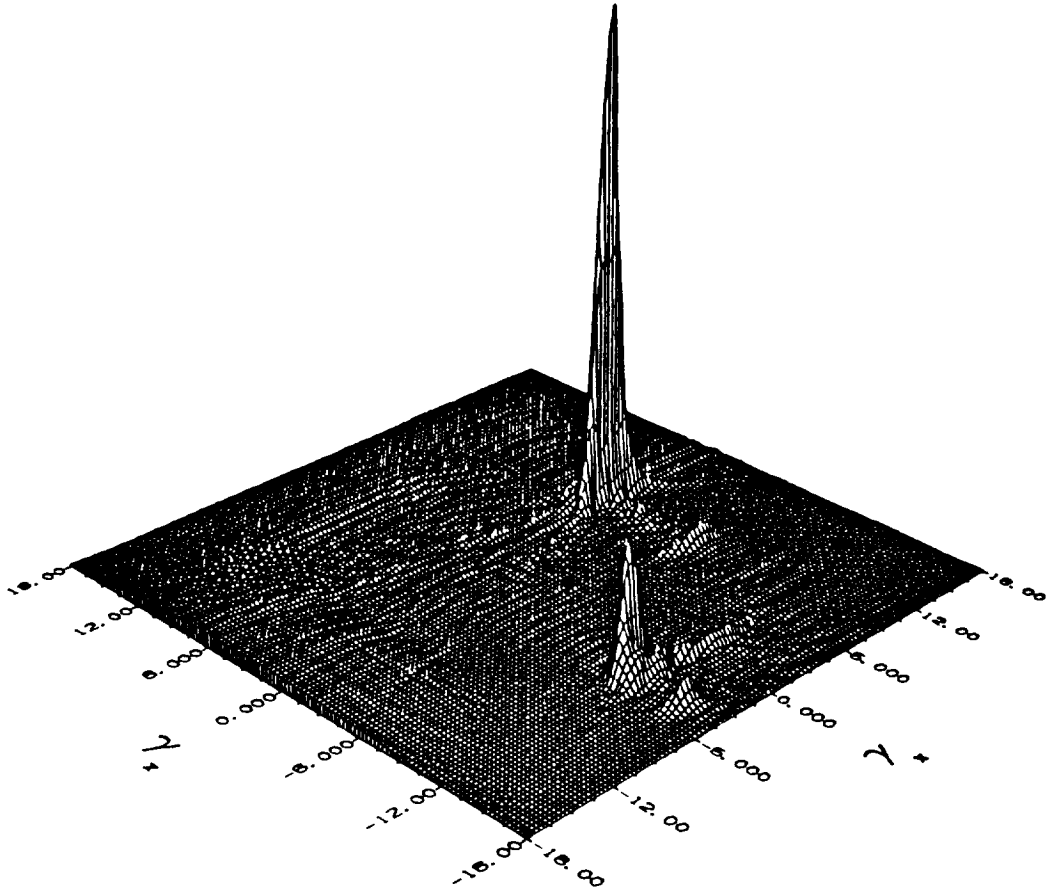


Figure 2.7: Surface plot of the images for the 6" and 3.25" spheres obtained from the backscattered fields.

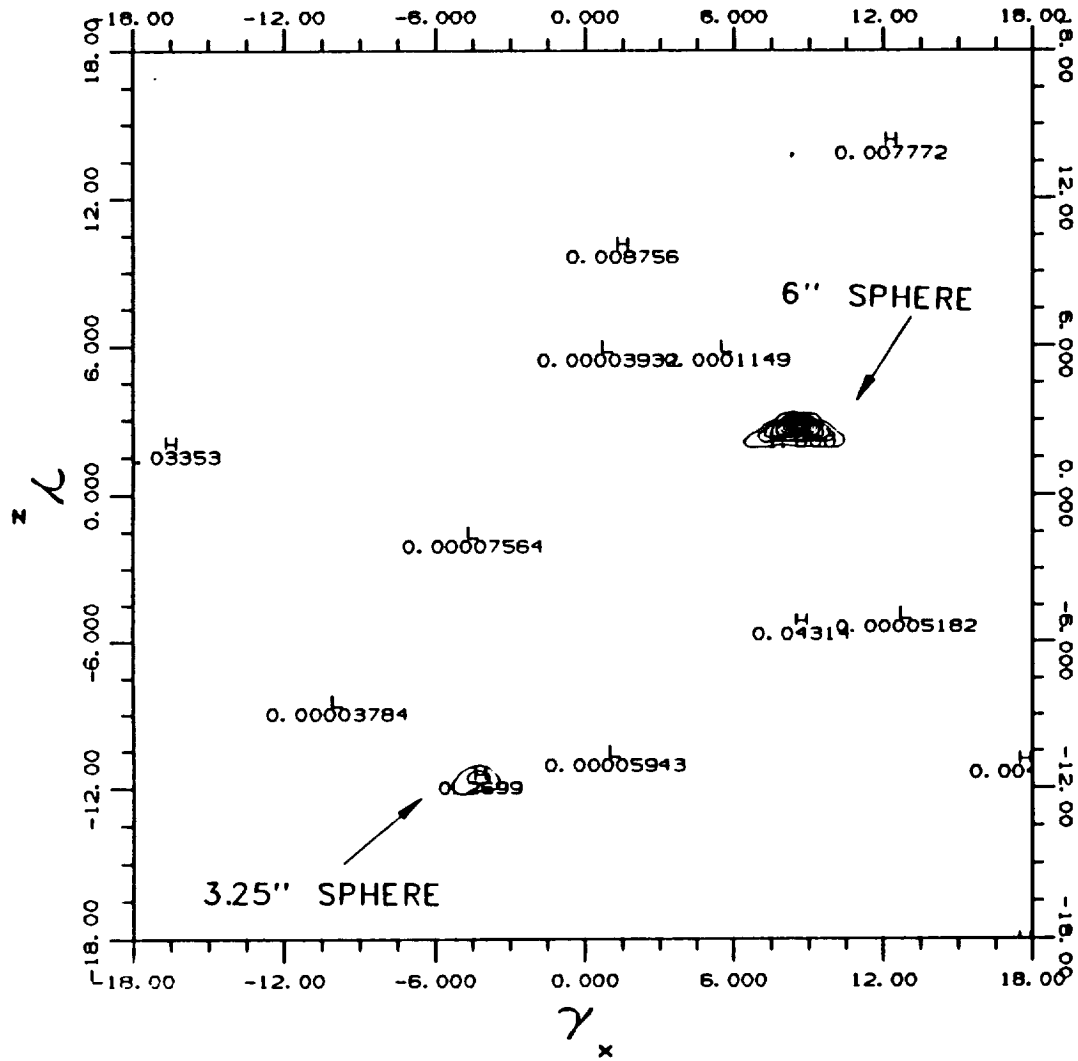


Figure 2.8: Contour plot of the images for the 6" and 3.25" spheres obtained from the backscattered fields.

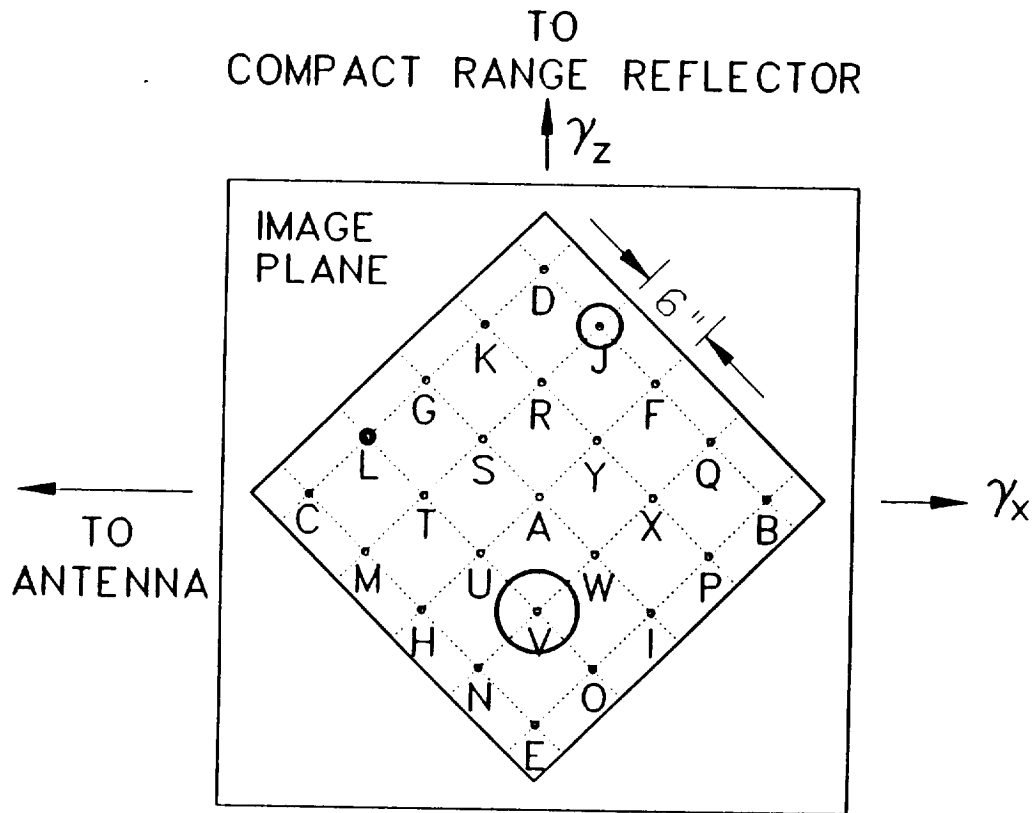


Figure 2.9: Positions of the 6", 3.25" and 1" spheres for the bistatic scattering measurement.

The second combination of the spheres used as the target is shown in Figure 2.9. Note that a 6" sphere is located at V, a 3.25" sphere at J, and a 1" sphere at L. The resulting images obtained from the bistatic scattered fields and backscattered fields are shown in Figures 2.10 to 2.13. Again, these images clearly show the scattering centers of the target and also the secondary scattering centers due to the creeping waves propagating around the spheres.

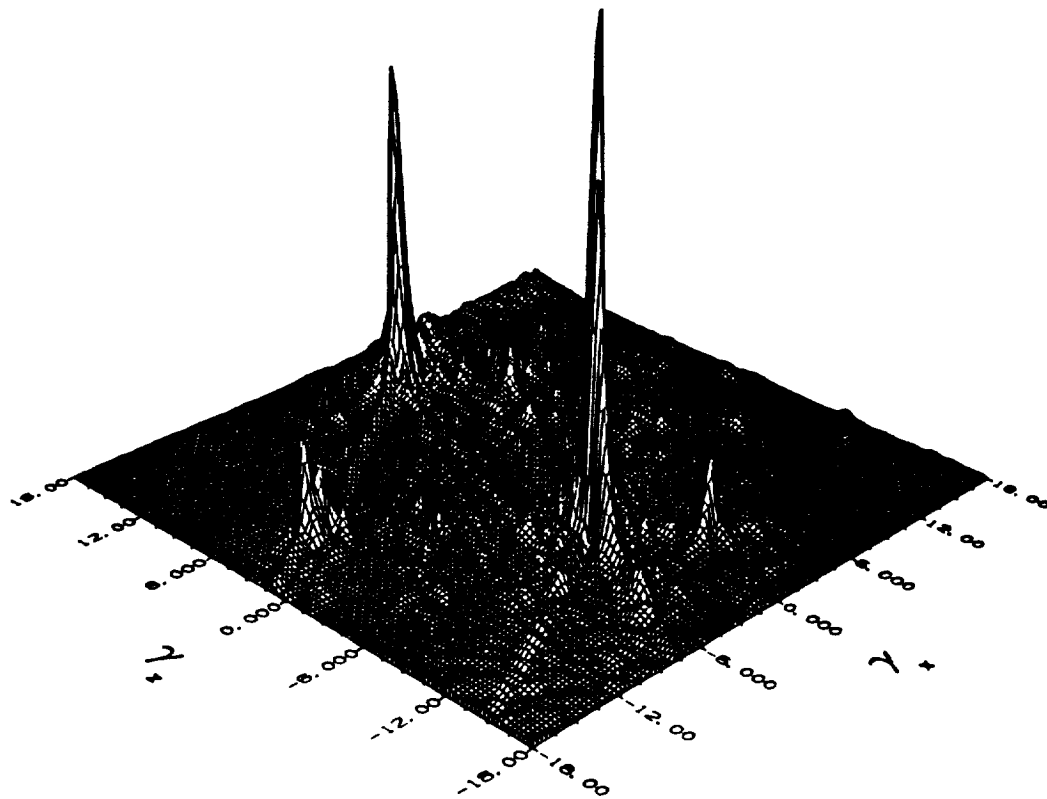


Figure 2.10: Surface plot of the images for the 6", 3.25" and 1" spheres obtained from the bistatic scattered fields.

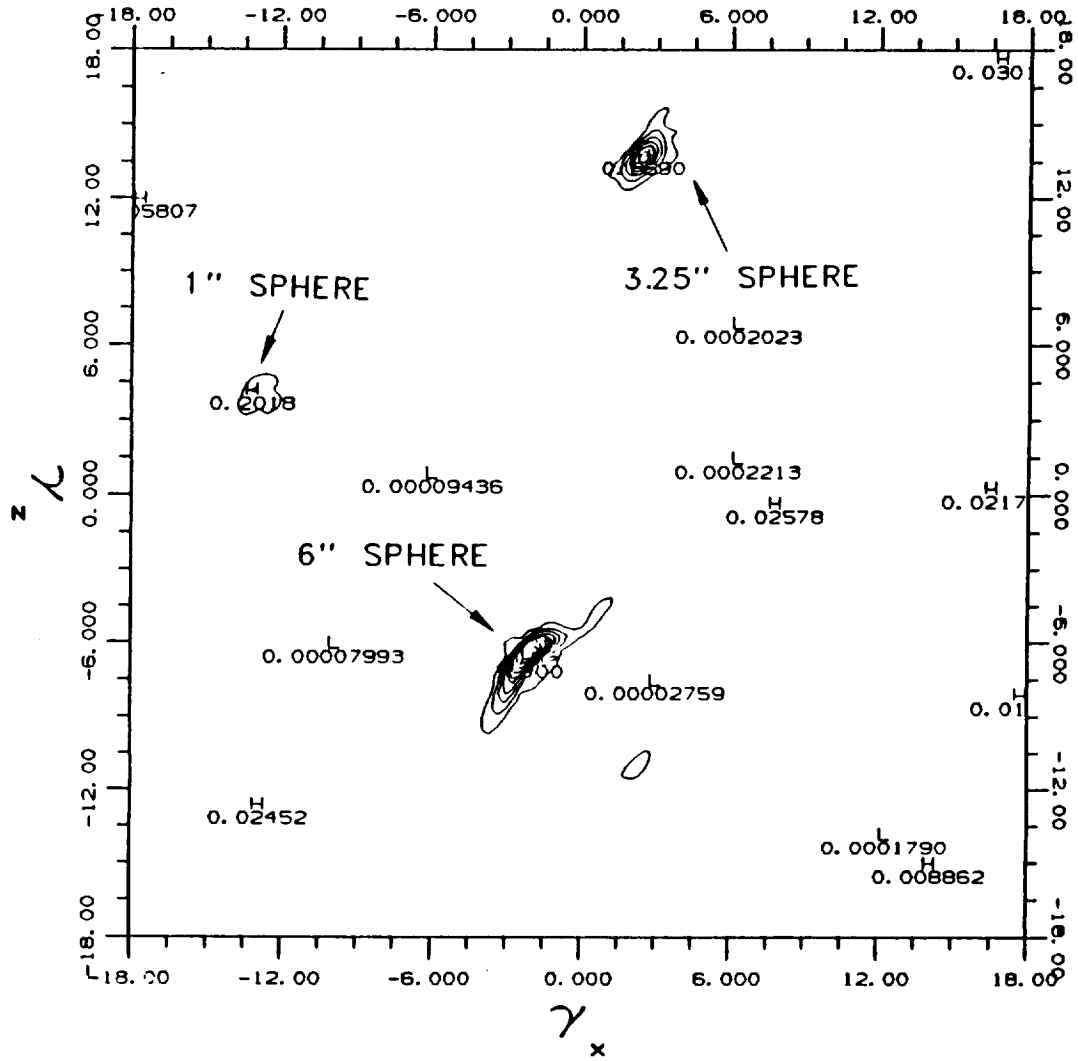


Figure 2.11: Contour plot of the images for the 6", 3.25" and 1" spheres obtained from the bistatic scattered fields.

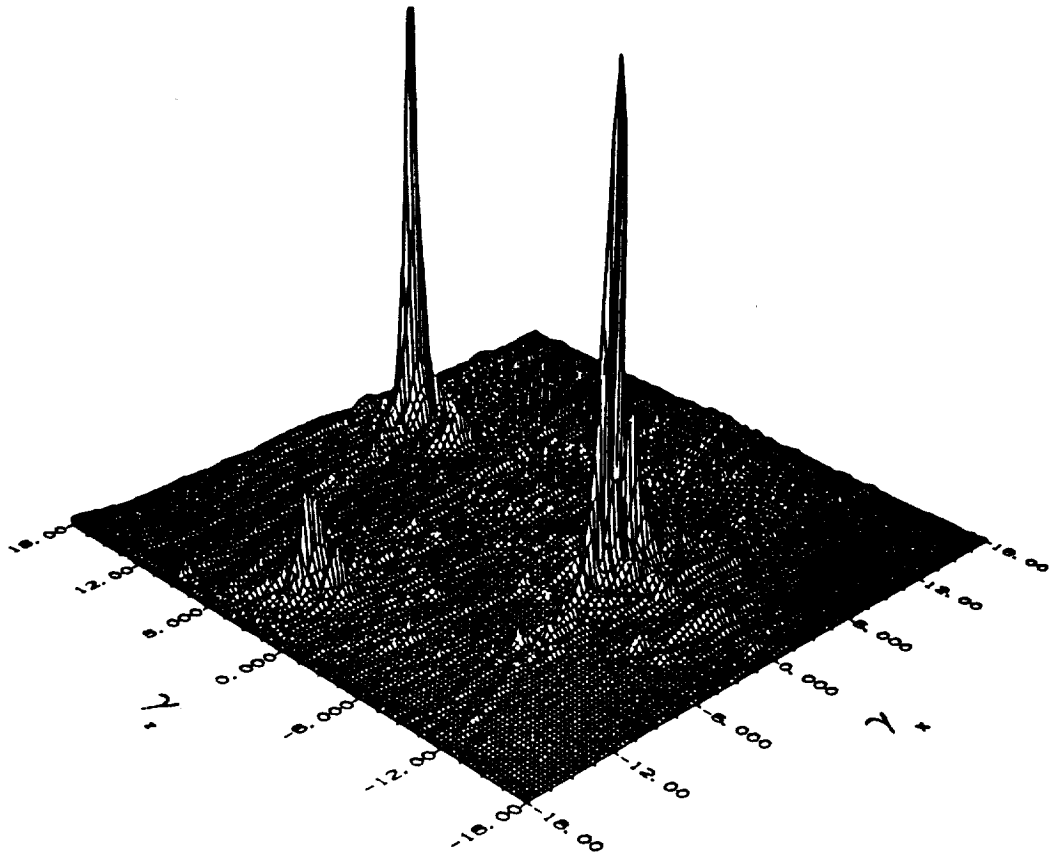


Figure 2.12: Surface plot of the images for the 6", 3.25" and 1" spheres obtained from the backscattered fields.



## **2.4 Summary and Conclusions**

An image processing technique using the bistatic scattered fields obtained in a compact range has been presented. Two compact ranges or one compact range and a horn antenna can be used to perform the bistatic scattering measurements. The antennas can be either focussed or defocussed. The bistatic scattered fields are then used to find the image, and consequently, the scattering centers of the target. The same processing approach can also be used to find the image of the target from backscattered fields. The processing technique does not require the target to be at far field of the antennas. Experimental results have been used to determine the images of various targets via this processing technique. Very good results have been obtained and presented.

## **2.5 Acknowledgement**

Numerical results presented in this report were made possible by a Grant (Project 355) from The Ohio Supercomputer Center, Columbus, Ohio.

# Chapter 3

## Target Signature Study

This is a brief review of the portion of the grant pertaining to target signature modeling over the period September 1, 1988 to February 28, 1989.

### 3.1 Introduction

The objective of this part is to determine and implement an effective method to integrate the use of UTD electromagnetic prediction codes for simulation of radar cross section into test and evaluation situations. UTD scattering code predictions can replace costly measurements. The signatures are used in the test loops to evaluate how effectively radar can follow targets. In this situation, it is necessary that the data be efficiently obtainable.

### 3.2 Scattering Code Overview

There is much scattering code development going on in the aircraft industry. These codes are primarily physical optics codes based on tiled or patched surfaces. They are used for component analysis and require large amount of computation times to do the integrations. Because they are based on physical optics, the specular points are

not explicitly defined. In addition, the some of the codes can be proprietary and/or very expensive.

A physical optics code is being developed by the U. S. Army Missile Intelligence Agency and Northrop called MISCAT. It is available inexpensively, however, it has the characteristic mentioned above and in addition has a more basic shape input capability. A new code is being developed called PGSCAT, which is a patch code for more general model descriptions, but again, it is PO based. Syracuse Research Corp. has a code that over comes the PO integration by using a scattering center description. There are no higher order terms involved and it uses basic shape models.

A different class of scattering codes are centered around the BRL modeling code. The BRL code is a CSG modeller for graphical representation of shapes. ERIM's SRIM code uses the BRL brute force ray shooting methods to reproduce synthetic aperture radar (SAR) images. It provides approximations to the fields as projections of the rays onto pixel planes. The ray shooting technique does find dihedral and trihedral speculars but it is extremely time consuming. GTRI has a RCS code similarly centered around the SAR concept. University of Illinois has taken the BRL ray tracing code and added a field capability to it. The resulting fields lack edge effects and is slow since it is based on PO and brute force ray tracing.

Another class of scattering codes deal with the near zone fusing problem. NWC has integrated the Ohio State University's NEC-BSC code into its applications for this purpose.

The suggested approach for test and evaluation purposes, is the use of a UTD based code such as the RCS - Basic Scattering Code [4]. It explicitly defines the specular, edge, and vertex diffraction points, as well as some higher order terms. It uses efficient ray tracing techniques based on the chosen geometry models. It does not need integrations since it uses closed form diffraction coefficients. This allows the flexibility to store the characteristics of the scattering centers of a target and then add the field information versus angle or frequency as they are needed. Since test and evaluation hardware in the loop situations need efficiency and flexibility of operation, this type of approach will be beneficial for large sized targets and the many angles of

approach needed. In addition, it has a bistatic scattering capability that might be useful in the future.

A study of the various UTD mechanisms that will be most important for modeling in the test and evaluation situation has been undertaken. Their theoretical characteristics have been studied from the point of view of obtaining the best way to determine, calculate and store each term individually. The UTD radar cross section prediction code, RCS-BSC version 2, has been modified so that its write algorithms for the UTD mechanisms calculated will better accommodate a volumetric output of the individual fields.

The RCS-BSC version 2 corner diffracted field section as been modified to allow access of an individual corner diffracted field instead of an edge in order to study which is the best way to store the fields in the data base. Other field sections will be modified as they are integrated into the data base.

An algorithm to access and plot the three dimensional field information in the data base has been started. This will allow a visual presentation of the fields in order to help determine the minimum sample rate for the different individual types of UTD mechanisms.

### 3.3 Storage Requirements

In order to better understand the size requirements of the data base needed for test and evaluation purposes the following simple examples illustrate the various possible configurations. It is assumed that the this information is for backscatter at a single frequency at this point. It is also assumed that a complete volumetric view of the object under consideration is needed with all polarization information.

For a full up unprocessed scattered field data base:

- $\theta pts = 1801$ ,  $\phi pts = 3601$ ,  $no. pols. = 4$
- Complex number = 8 bytes, step size =  $0.1^\circ$
- Storage required = 207 megabytes

For a full up processed data base, that is with a median average representation of the fields:

- $\theta pts = 91, \phi pts = 181, no. polys. = 4$
- Complex number = 8 bytes, step size =  $2^\circ$
- Storage required = 0.527 megabytes

The median average of the fields is not necessarily desirable, however, for test and evaluation purposes since the scintillation of the fields is useful to test radar performance. In addition, the processed data base can not be used for imaging since the phase information is lost.

For individual dominant terms only, it can be assumed that the sampling rate can be greatly reduce so that:

- $\theta pts = 37, \phi pts = 73, no. polys. = 4$
- Complex number = 8 bytes, step size =  $5^\circ$
- Storage required per term = 0.086 megabytes

This implies that approximately 10–20 terms can be used and still have the storage and more field information content than the processed data base. A few thousand terms can be stored and have the same information as the full up unprocessed data base. Actually some of the storage would be needed for several frequencies. This, however, appears to be the best alternative.

One more possible solution has been investigated. This entails storing scattering centers only and then post processing the fields. The storage of the scattering centers locations only turns out to be very complicated since the terms can be shadowed or they can move versus incident and observation direction. In addition, there will be a trade off between storage and speed of retrieval which will reduce its desirability for real time test and evaluation purposes.

In summary:

- Full up unprocessed data base requires large amounts of storage.
- Processed data base loses local variations of signals.
- Processed data base can not be used for imaging.

- Individual dominant terms can be reconstructed to give the same information as full up unprocessed data base with less storage.
- Need for multiple frequency information further compounds full up data storage.
- Individual terms data base will still greatly reduce storage requirements.
- One, two or three dimensional imaging possible.

### **3.4 Further Work**

Test cases, that will represent meaningful situations for test and evaluation purposes, are being determined to validate the algorithms being developed. Simple scattering shapes will be used such as plate and cone frustums to test the basic ideas. A model of a QF-100 aircraft has been suggested by K. Oh and C. L Yu at Pacific Missile Test Center, since they have measured data on a one fourth scale model.

# Chapter 4

## Aircraft Code Study

This is a brief review of the portion of the grant pertaining to modifications to the aircraft and missile antenna code over the period September 1, 1988 to February 28, 1989.

### 4.1 Introduction

The purpose of this effort is to modify the aircraft and missile antenna code [5] to provide simple models for rectangular microstrip patches and to add a smoothing algorithm for radiation pattern presentation. In addition, a study to implement the aircraft code on a personnel computer will be initiated.

### 4.2 Smoothing Algorithm

The existing Ohio State University Aircraft code (NEWAIR3) [5] has been modified so that any spikes in the radiation patterns are removed by a smoothing algorithm. The input data is as follows:

EX:  
LSMOOTH, NAVG, SEN

where

LSMOOTH = T, spikes are removed from the output data  
F, the output data is not modified

NAVG = # of data points used to compute an average.  
It is always even, usually NAVG=4.

SEN = # of standard deviations that is allowed before a  
spike is removed. SEN does not have to be an integer.

### 4.3 Patch Antenna

Another task that is near completion is the addition of a simple model for a rectangular microstrip patch. The patch is modeled by a pair of short magnetic monopoles which is accurate when the lowest order (1,0) mode is excited in the patch. The input data of the NEWAIR3 code (in the SG: command) has been slightly modified to input the parameters for the rectangular patch.

### 4.4 PC Study

A study to implement the NEWAIR3 on a personnel computer has been initiated. Additional memory and software has been obtained to start the task on an IBM compatible clone. This work will be continuing during the next phase.

# Chapter 5

## SATCOM Antenna Study

This is a brief review of the portion of the grant pertaining to satellite communication antenna (SATCOM) modeling over the period from the start of this part December 1, 1988 to February 28, 1989.

### 5.1 Introduction

The purpose of this effort is to study the performance of SATCOM antennas on aircraft. The potential locations of the antenna system for best pattern and polarization coverage is being assessed on an P3C aircraft. A circular polarized antenna composed of crossed dipoles is being considered. The aircraft is being modeled using a computer code based on the Uniform Geometrical Theory of Diffraction (UTD) which is the NEC-BSC V3.1 [6].

### 5.2 Batwing Antenna

The first phase has been to analyze the present candidate UHF SATCOM antenna system and its location on a P3C aircraft using the NEC-BSC. Naval Air Test Center has provided the antenna system information which is a Dorne and Margolin DM 1501341 (Batwing) airborne UHF satellite communication antenna as shown in Figure 5.1.

A simple crossed dipole has been used in the code with the corresponding dimensions given in the figure. All the results have been referenced to a circular polarized isotropic radiator. The calculated result in Figure 5.2 at 244 MHz can be compared with the measured result supplied by the manufacturer in Figure 5.3 for the antenna on a 8 foot ground plane in the principal elevation cut for the antenna. The results compare very well. In order to test the NEC-BSC's representation of the antenna for a pattern taken along the length of one of the dipole arms, the pattern at 300 MHz in Figure 5.4 can be compared with a method of moments result [7] in Figure 5.5. Again quite good agreement is obtained.

### 5.3 Model Validation

Naval Air Test Center has supplied extensive model measurements independently conducted by Boeing on a 1/17 scale model and Lockheed on a 1/10 scale model. The Boeing data is used to validate the model here. The antenna is located as illustrated in Figure 5.6, which also shows the computer model used to generate the results. The calculated results for 300 GHz are compared with measurements for the roll plane in Figures 5.7 and 5.8, for the azimuth plane in Figures 5.9 and 5.10, and for the elevation plane in Figures 5.11 and 5.12 all for right hand polarization. The cross polarized fields are compared for the roll plane in Figures 5.13 and 5.14, for the azimuth plane in Figures 5.15 and 5.16, and for the elevation plane in Figures 5.17 and 5.18 all for left hand polarization. Notice that the roll plane results compare very well. The azimuth and elevation results, however, have about a 10 dB difference near the horizon. This will be investigated further, but overall the agreement is good.

### 5.4 Further Work

In the next phase, a study of alternative antenna locations and possibly alternative systems to provide a minimum of 330° azimuth, from

**OUTLINE DIMENSIONS**  
Inches (Centimeters)

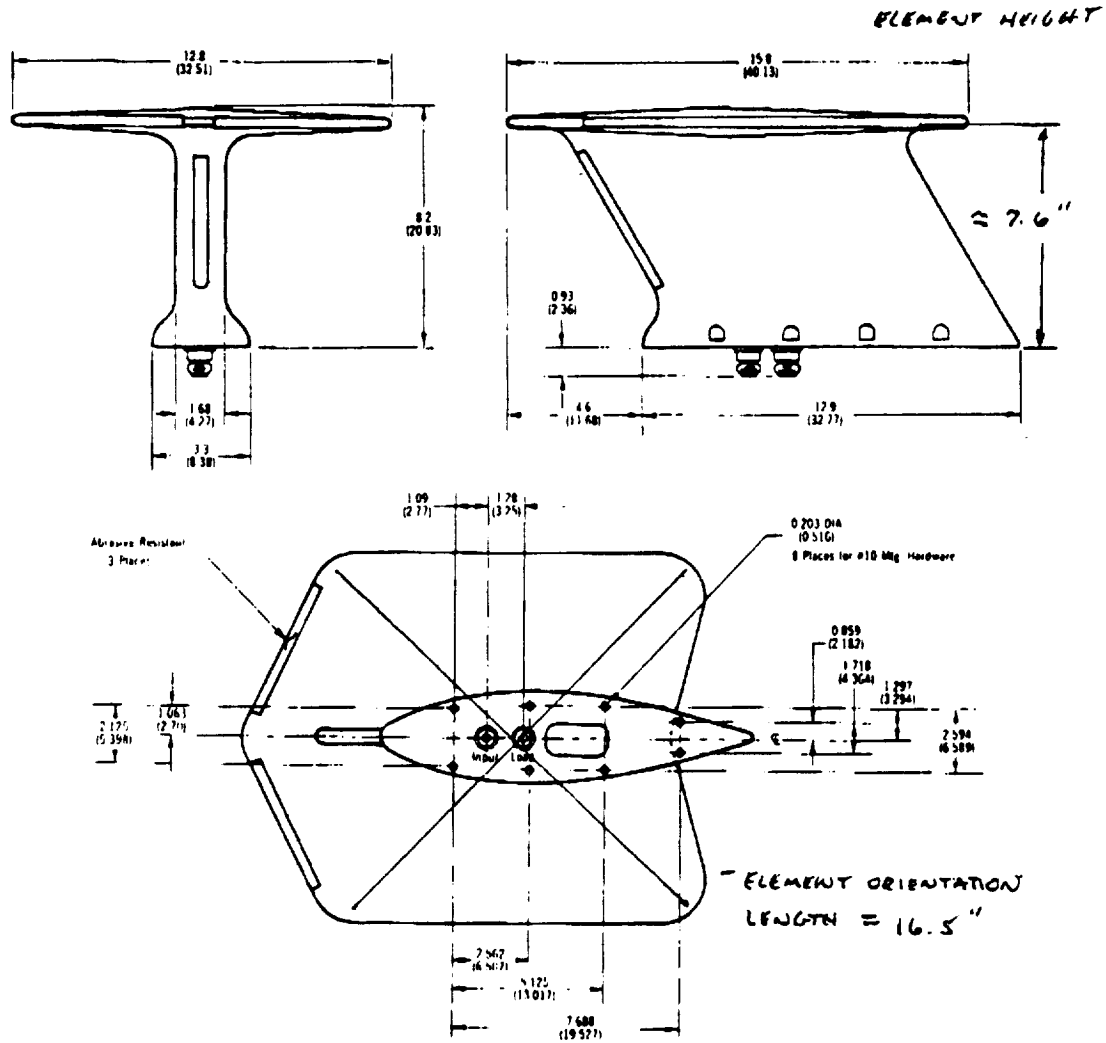


Figure 5.1: Batwing airborne UHF satellite communication antenna of Dorne and Magolin.

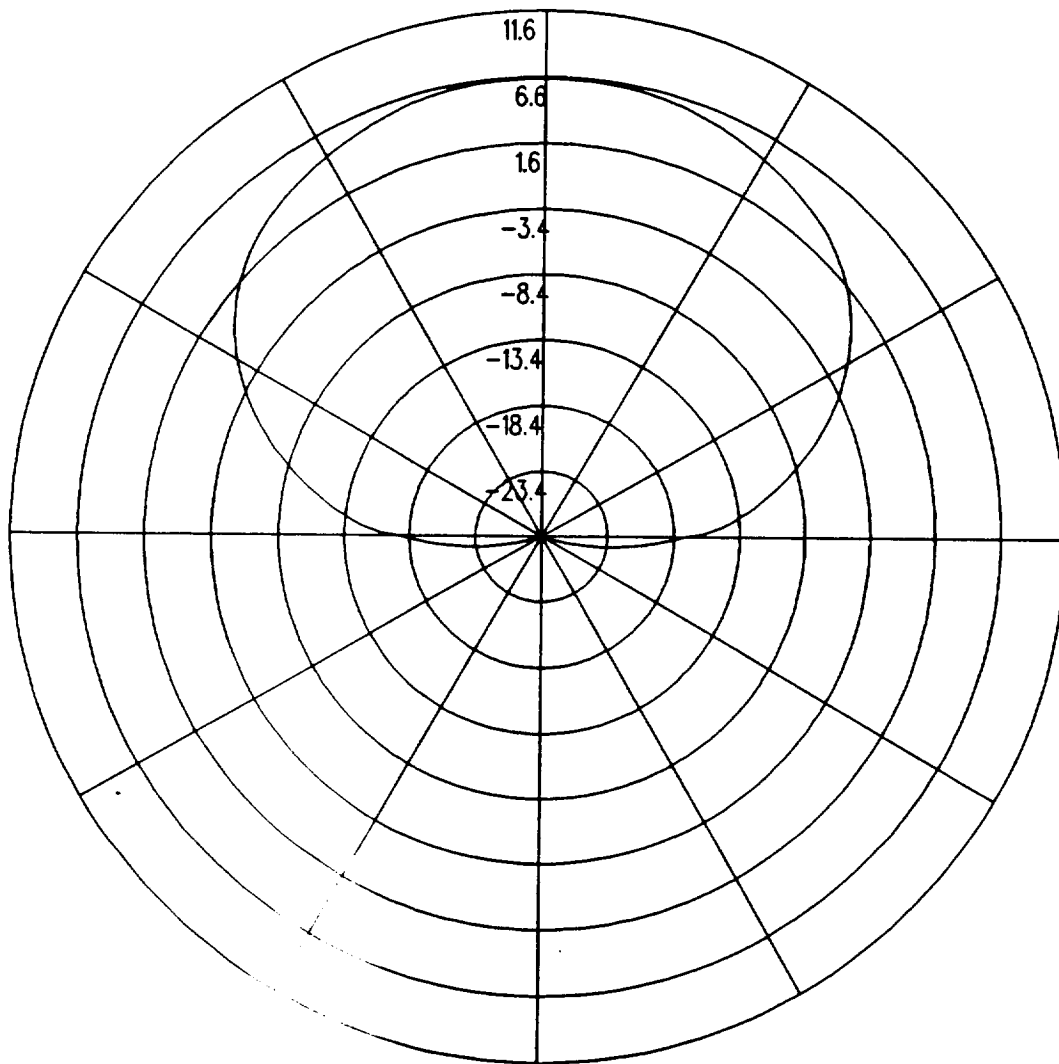
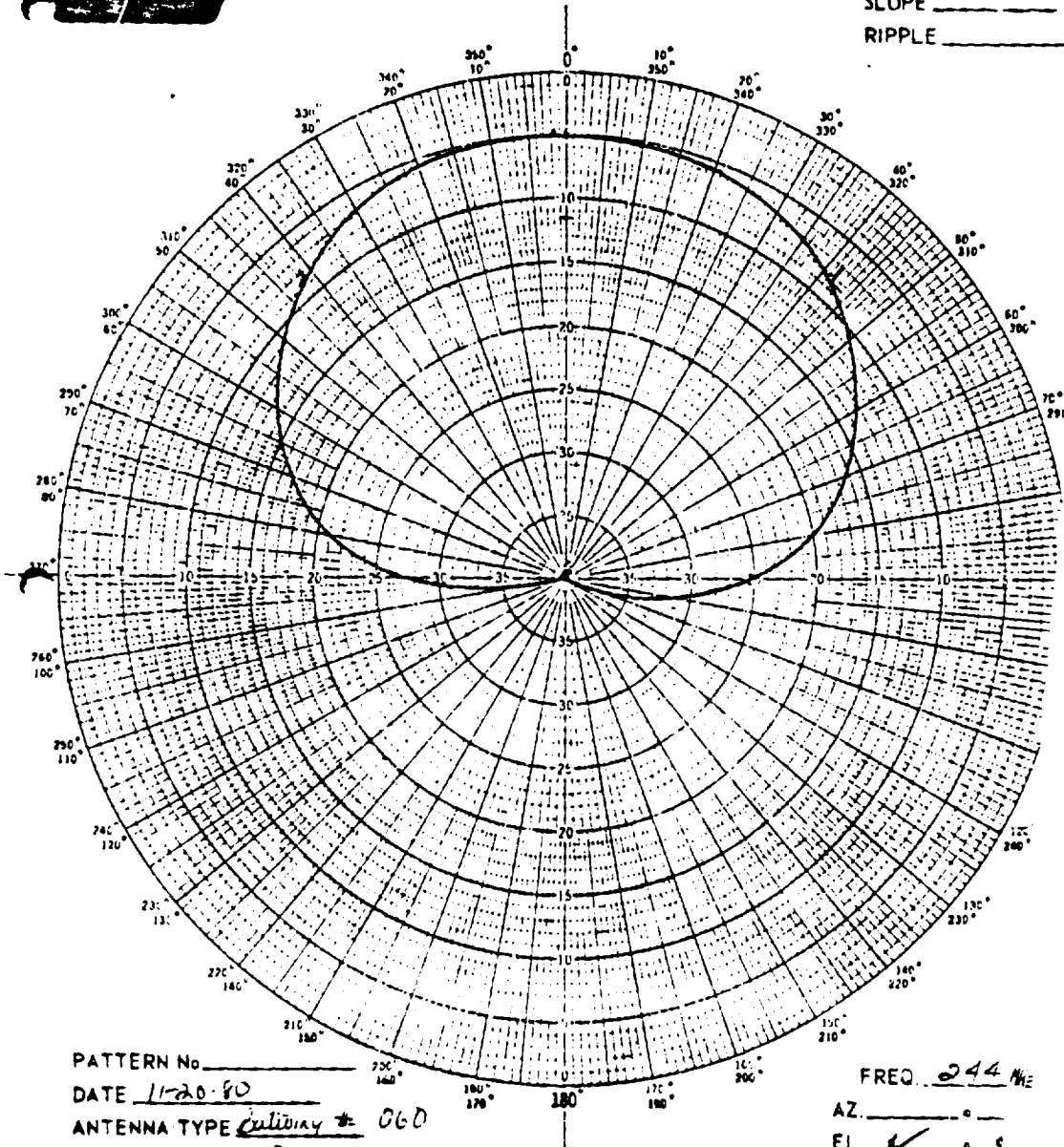


Figure 5.2: Calculated Batwing right hand circular polarized antenna pattern at 244 MHz on an 8' ground plane using the NEC-BSC.



CP ISOTROPK LEVEL - 11.6 db

BW \_\_\_\_\_  
SQUINT \_\_\_\_\_  
BACKLOBE \_\_\_\_\_  
SLOPE \_\_\_\_\_  
RIPPLE \_\_\_\_\_



PATTERN No \_\_\_\_\_  
DATE 11-20-80  
ANTENNA TYPE colinear # 060  
PATTERN RANGE 2  
TAKEN BY MM 1M

FREQ 244 MHz  
AZ. \_\_\_\_\_  
EL. ✓  
POLARIZATION ✓

Figure 5.3: Measured Batwing right hand circular polarized antenna pattern at 244 MHz on an 8' ground plane. (Pattern supplied by Dorne and Margolin.)

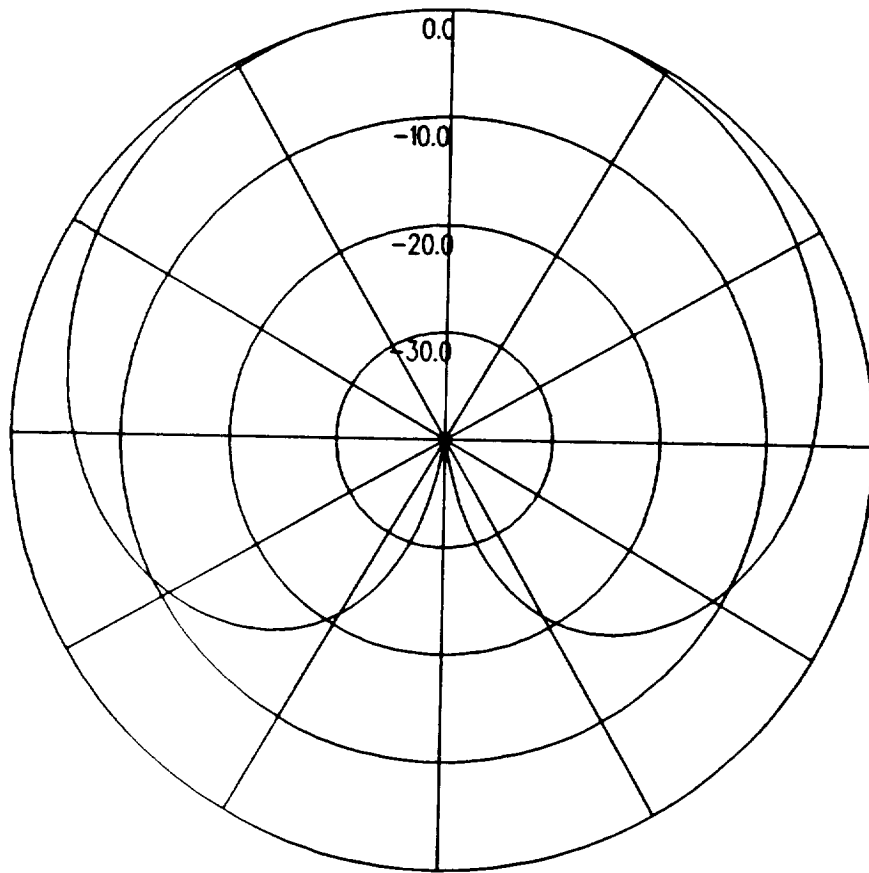


Figure 5.4: Calculated Batwing right hand circular polarized antenna pattern at 300 MHz on an infinite ground plane using the NEC-BSC.

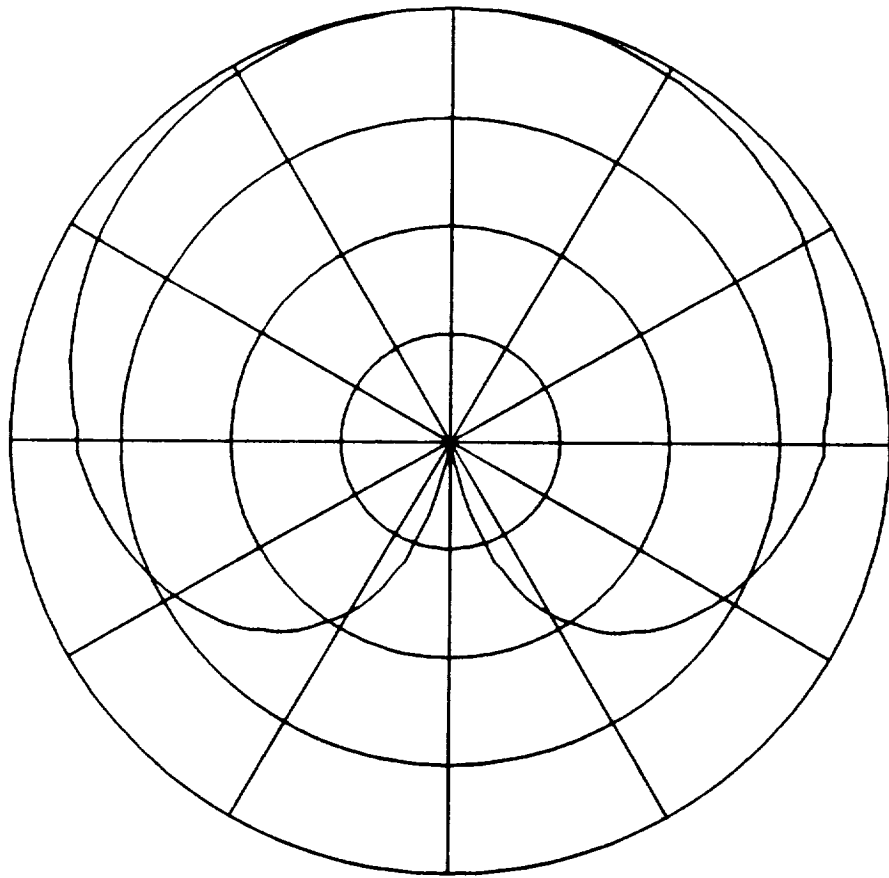


Figure 5.5: Calculated Batwing right hand circular polarized antenna pattern at 300 MHz on an infinite ground plane using the ESP code.

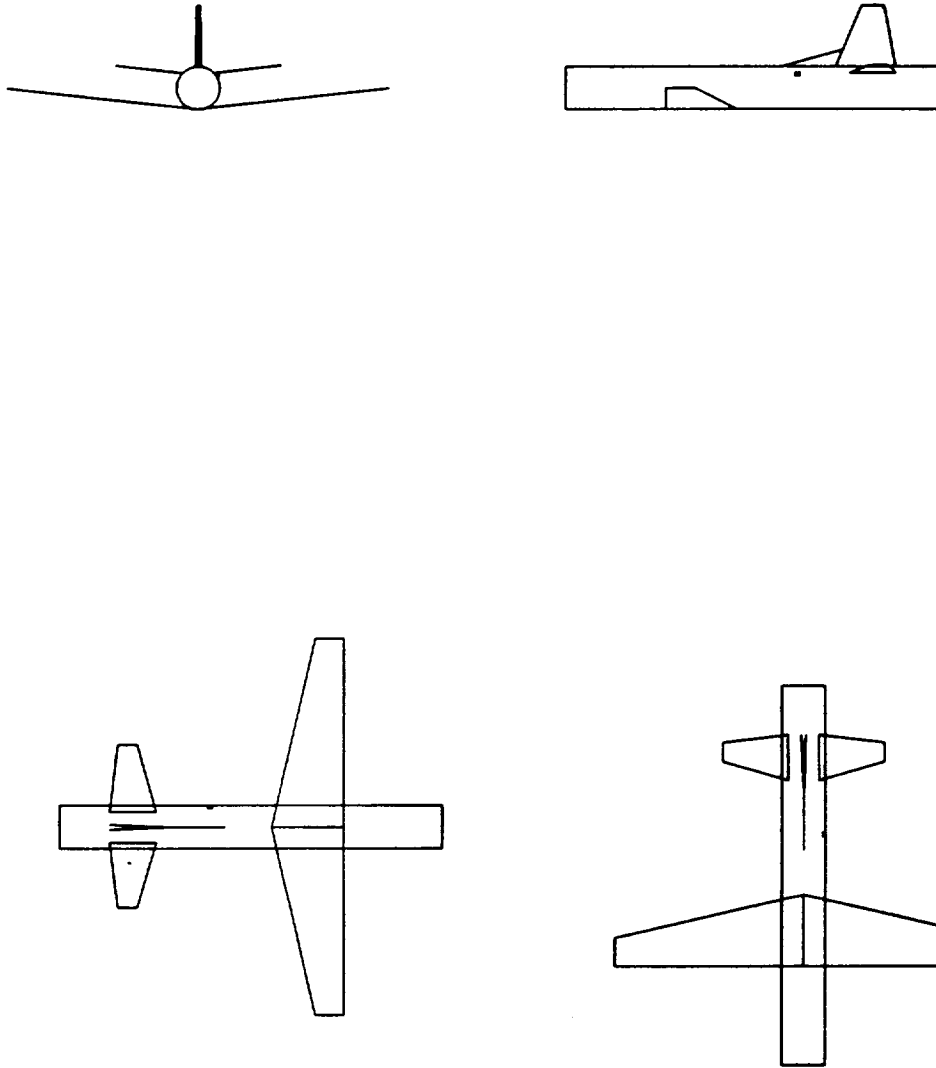


Figure 5.6: Geometry of the model of the P3C aircraft code used in the NEC-BSC showing the location of the antenna.

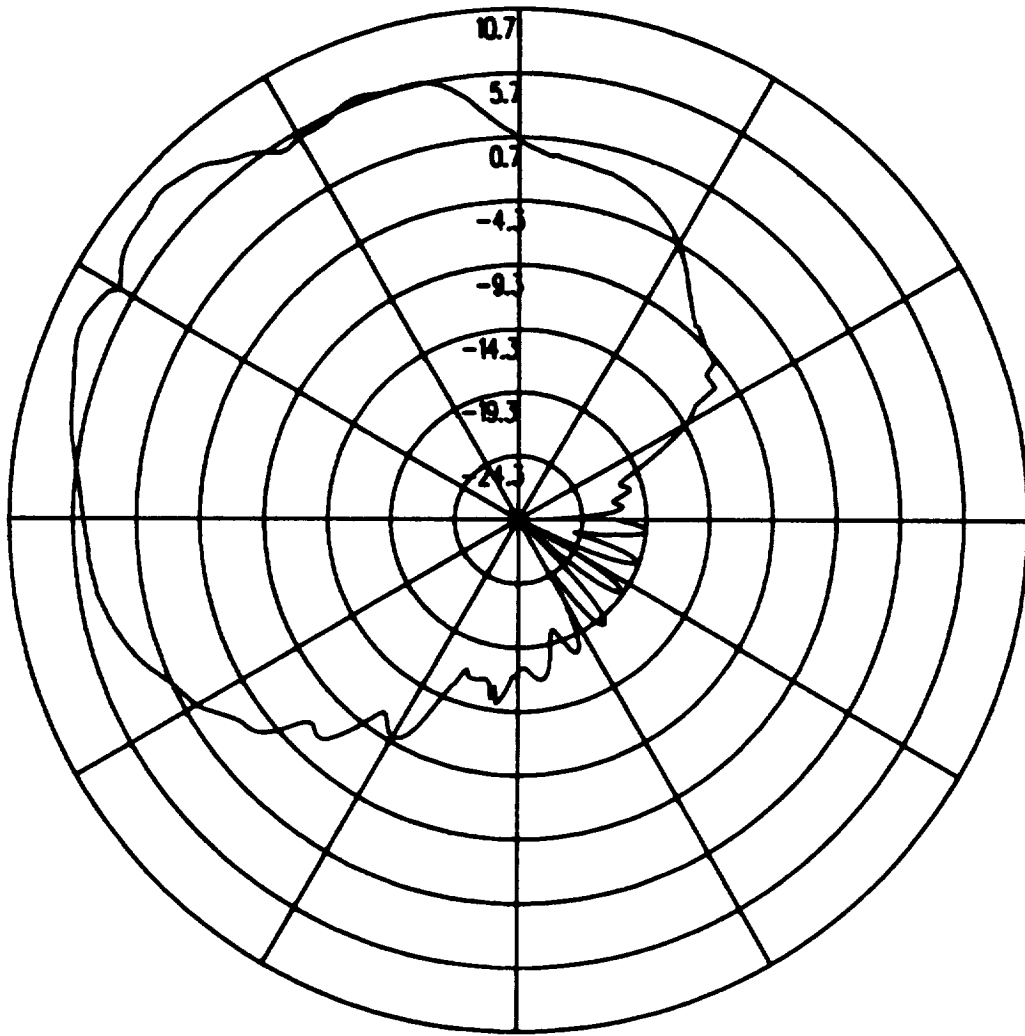


Figure 5.7: UTD calculated roll plane pattern for batwing antenna on a P3C for right hand circular polarization in the roll plane at 300 MHz.



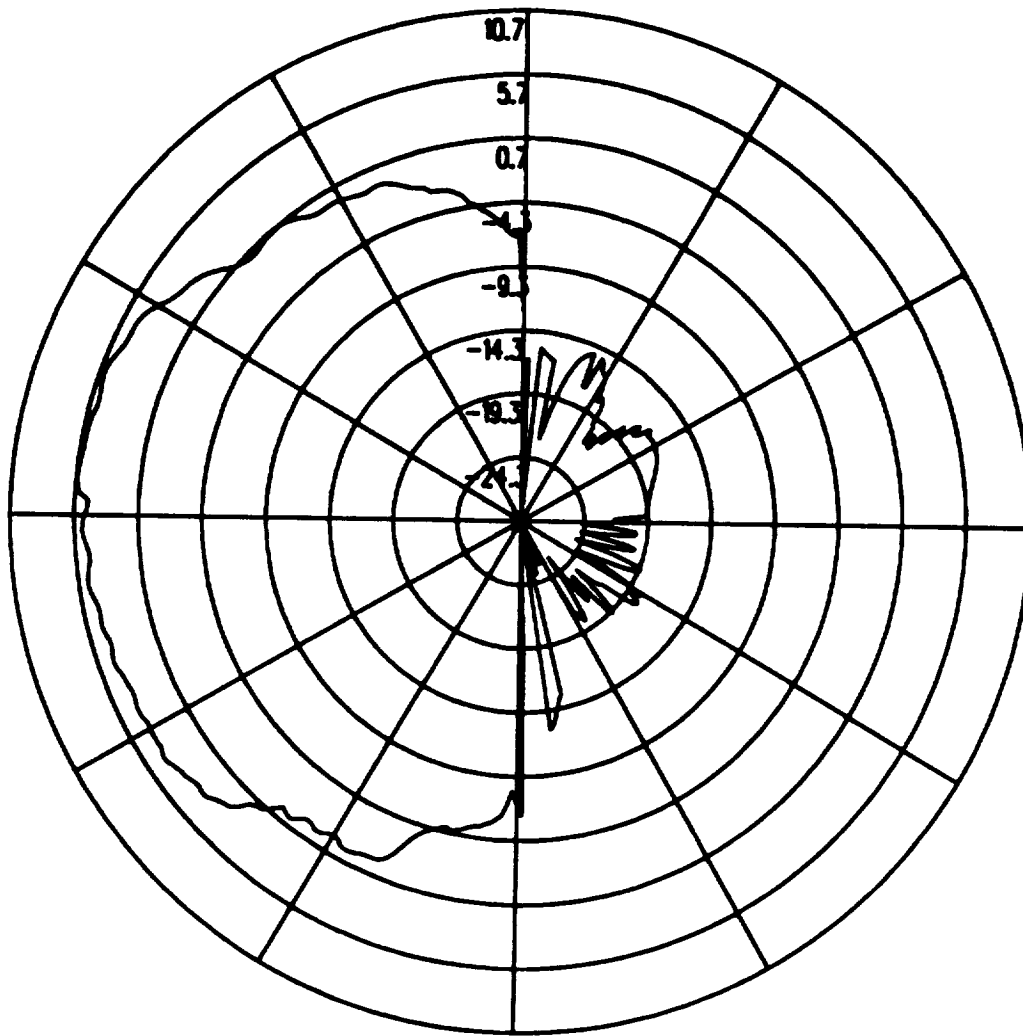


Figure 5.9: UTD calculated azimuth plane pattern for batwing antenna on a P3C for right hand circular polarization in the roll plane at 300 MHz.



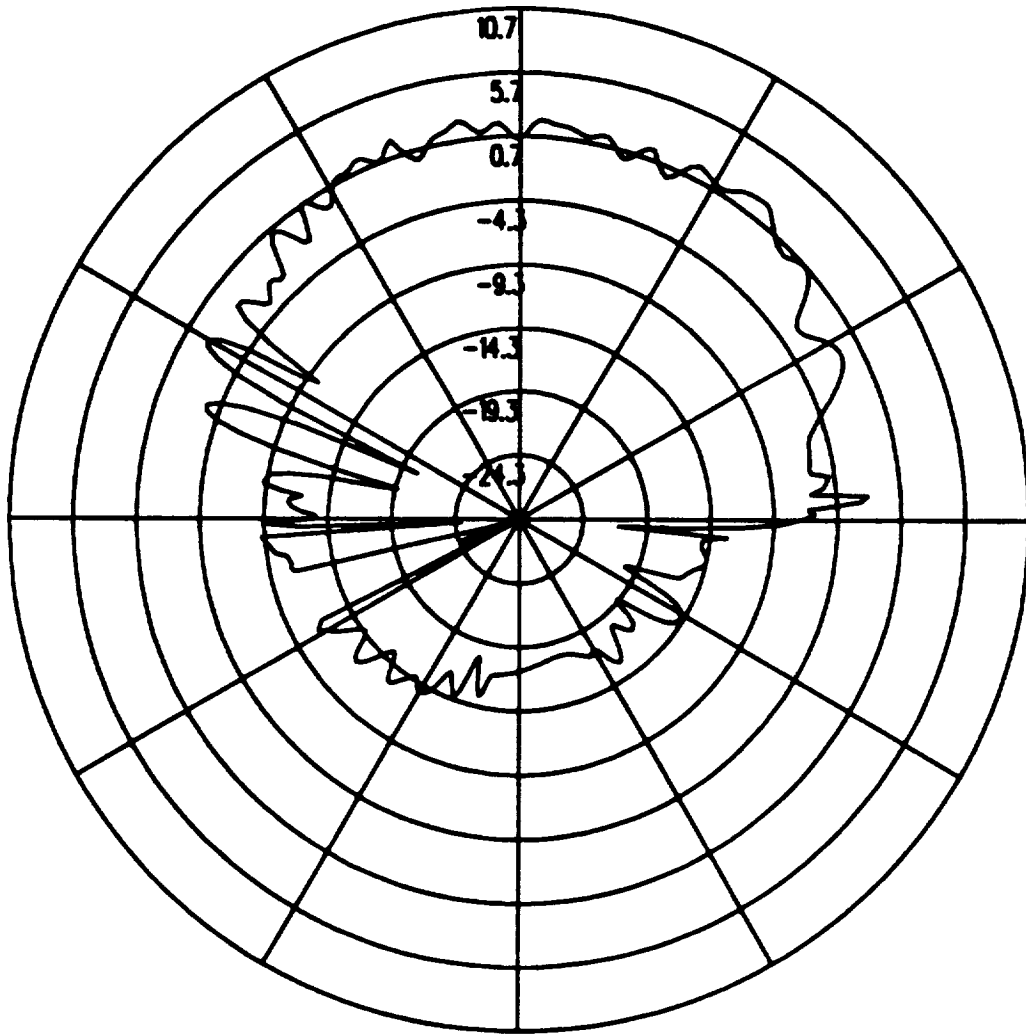


Figure 5.11: UTD calculated elevation plane pattern for batwing antenna on a P3C for right hand circular polarization in the roll plane at 300 MHz.

ORIGINAL PAGE IS  
OF POOR QUALITY

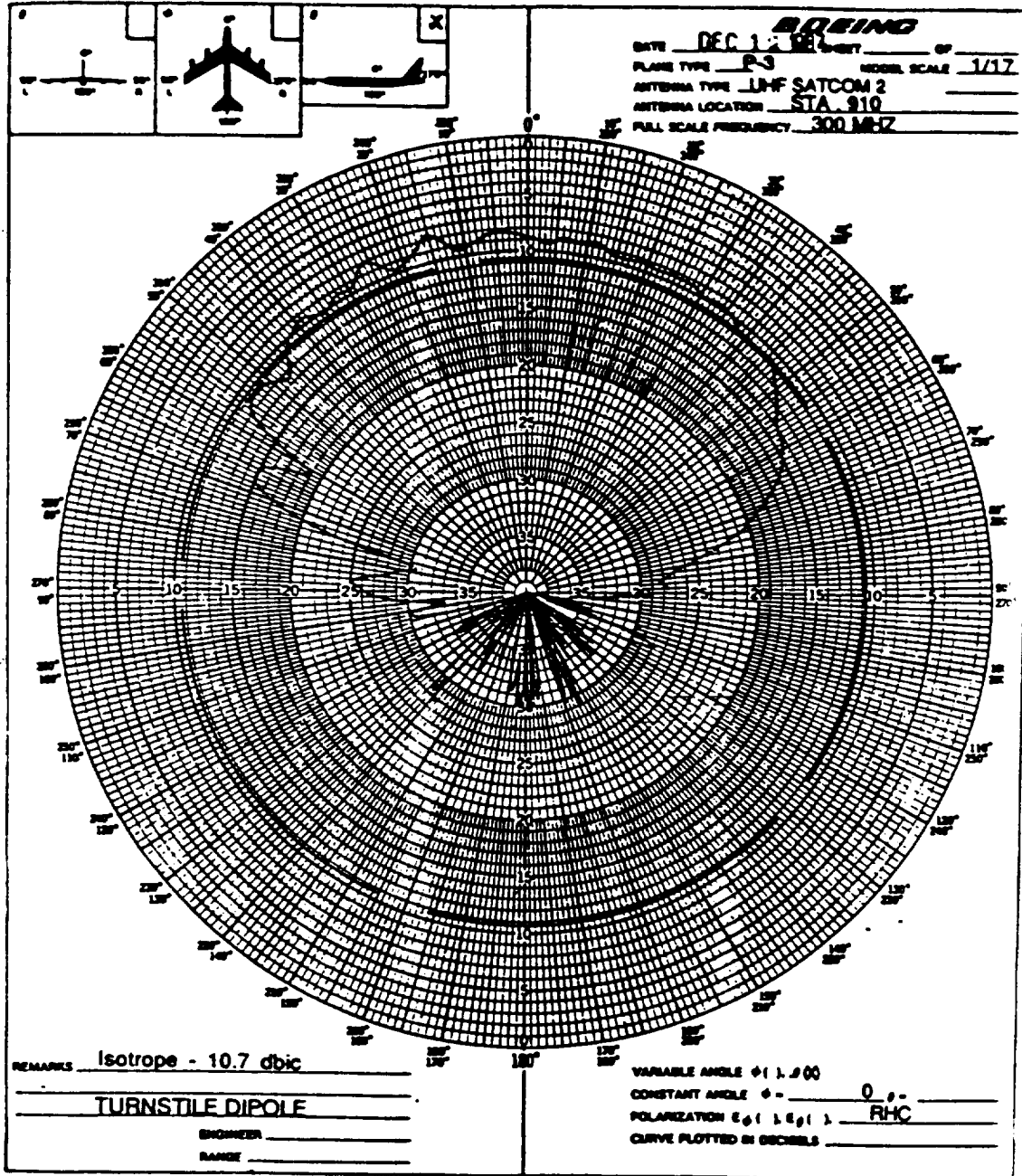


Figure 5.12: Boeing's measured elevation plane pattern for batwing antenna on a P3C for right hand circular polarization in the roll plane at 300 MHz.

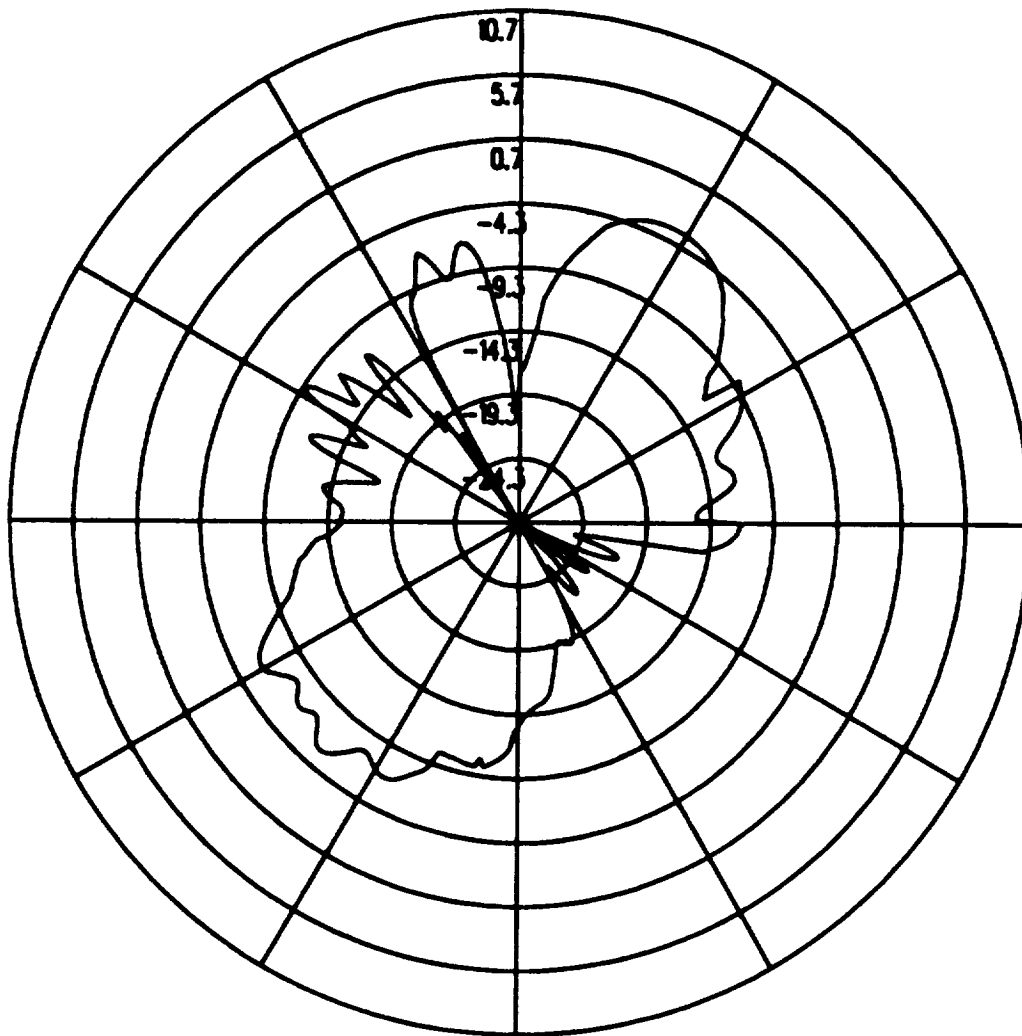


Figure 5.13: UTD calculated roll plane pattern for batwing antenna on a P3C for left hand circular polarization in the roll plane at 300 MHz.

ORIGINAL PAGE IS  
OF POOR QUALITY

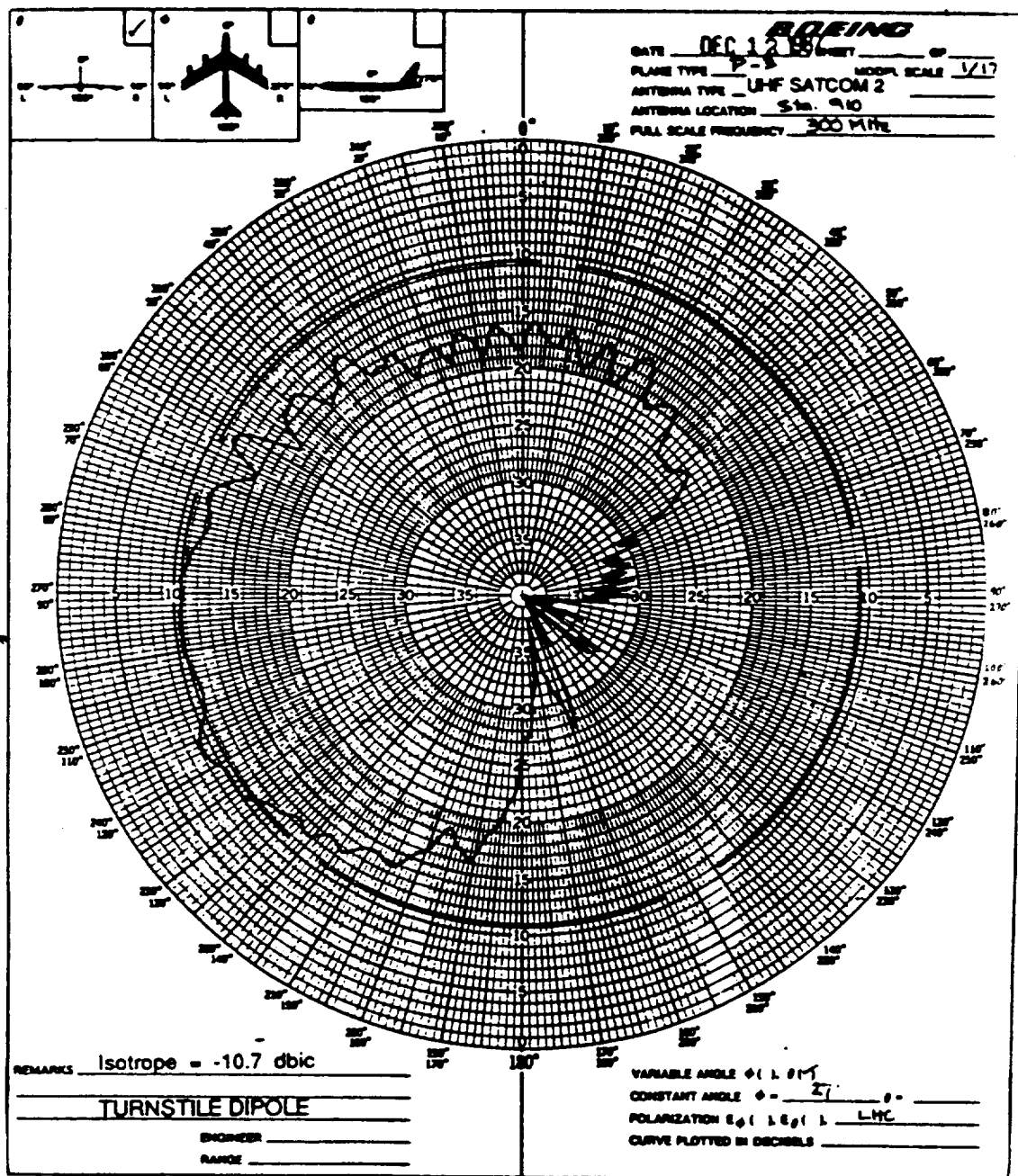


Figure 5.14: Boeing's measured roll plane pattern for batwing antenna on a P3C for left hand circular polarization in the roll plane at 300 MHz.

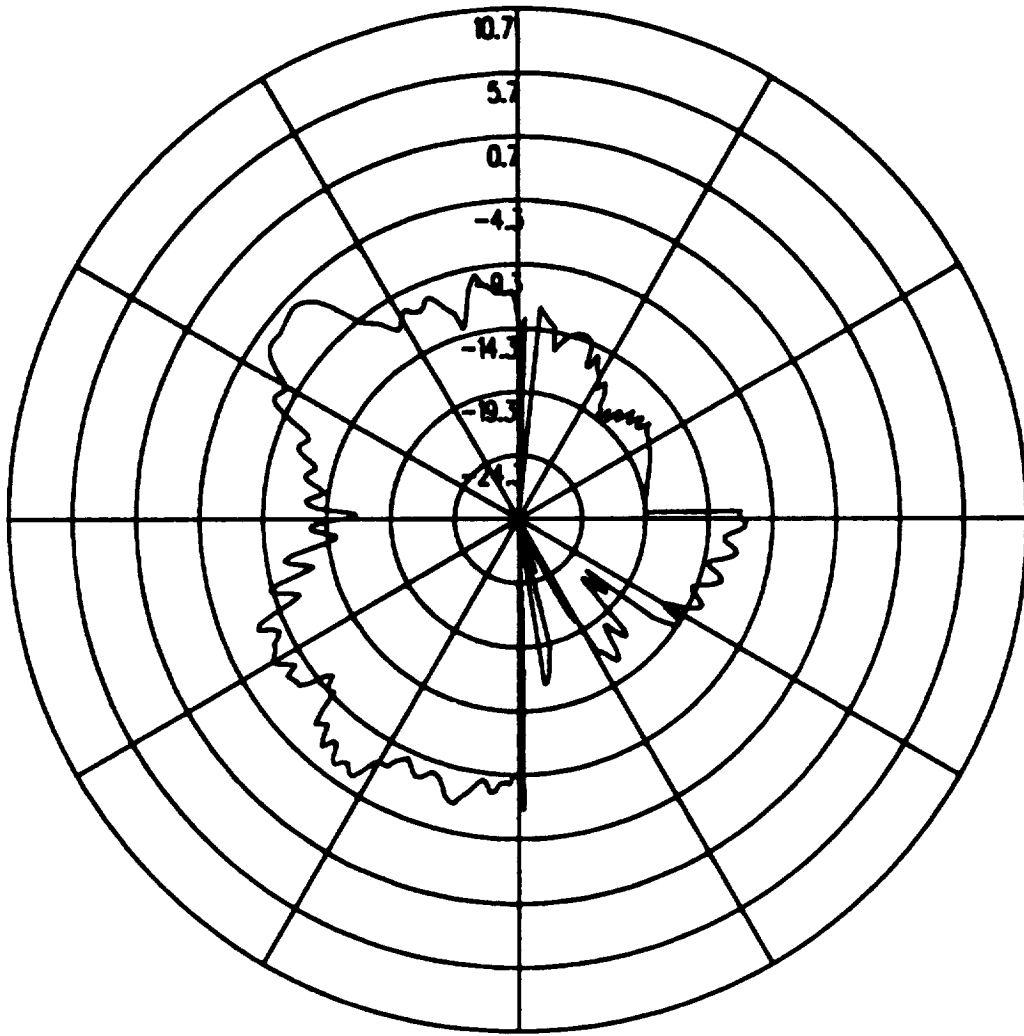


Figure 5.15: UTD calculated azimuth plane pattern for batwing antenna on a P3C for left hand circular polarization in the roll plane at 300 MHz.



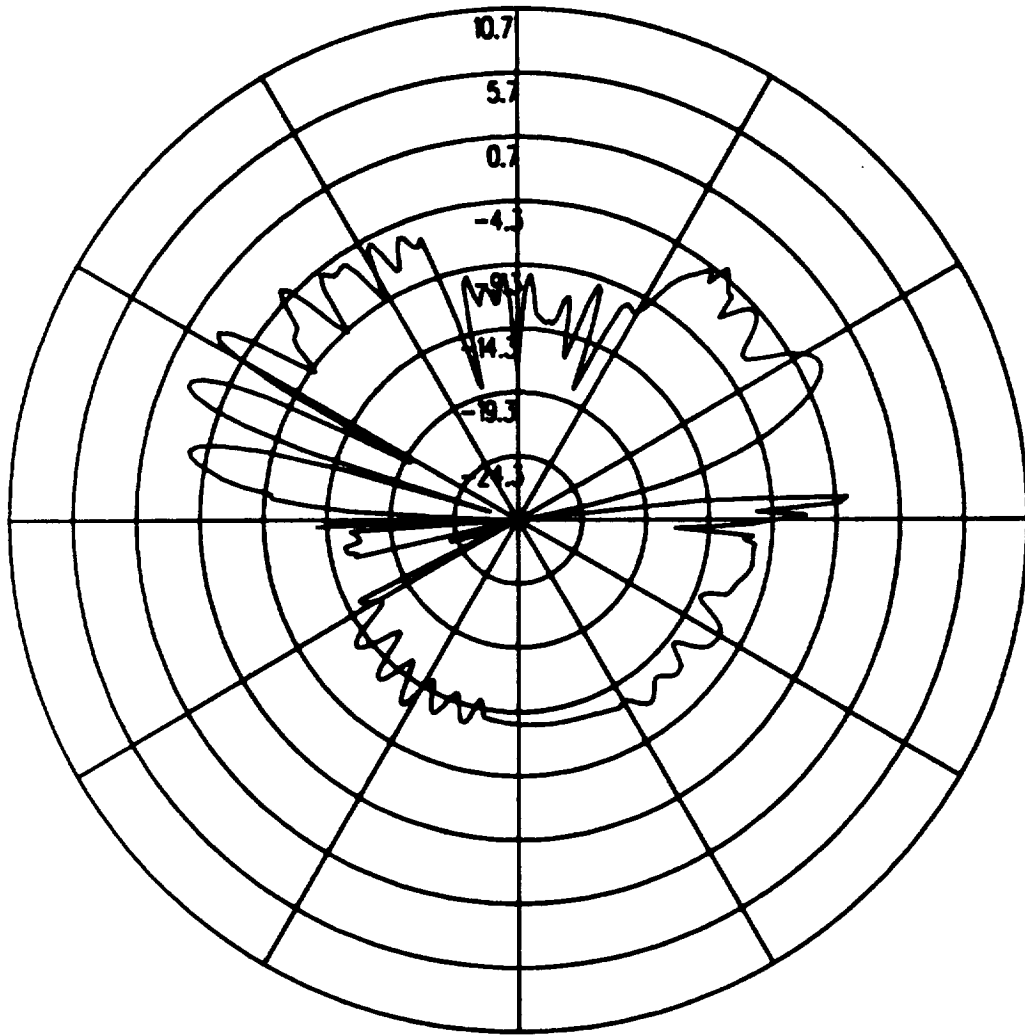


Figure 5.17: UTD calculated elevation plane pattern for batwing antenna on a P3C for left hand circular polarization in the roll plane at 300 MHz.

ORIGINAL PAGE IS  
OF POOR QUALITY

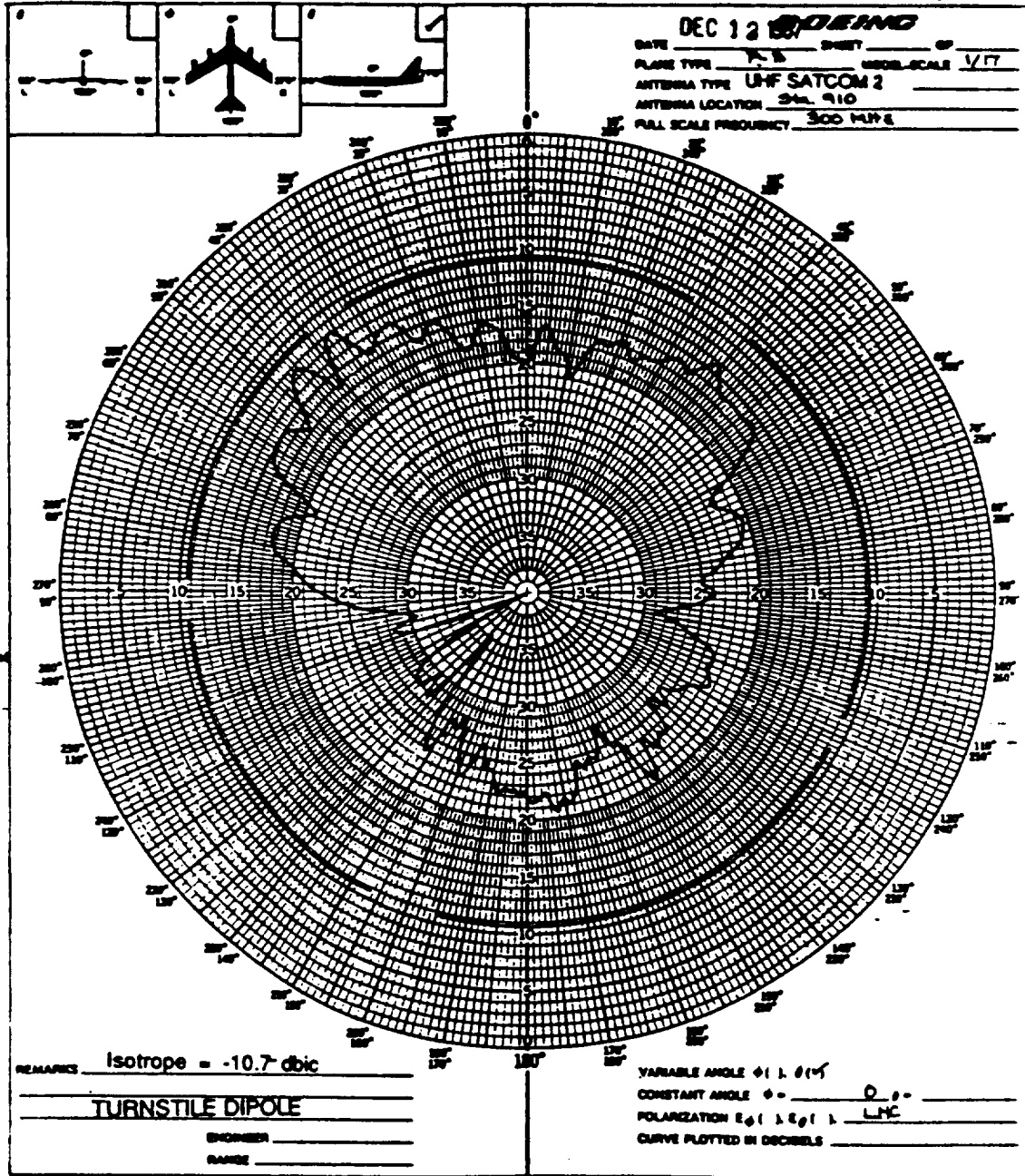


Figure 5.18: Boeing's measured elevation plane pattern for batwing antenna on a P3C for left hand circular polarization in the roll plane at 300 MHz.

zenith to  $10^\circ$  above aircraft horizon will be undertaken. The antenna system must provide performance to maintain the satellite link in areas of high signal fading to multipath effects. This will primarily be accomplished with the use of the same antenna mentioned above by exploring alternative locations around the aircraft.

# Bibliography

- [1] D. L. Mensa, *High Resolution Radar Imaging*. Artech House, Inc, 1981.
- [2] D. L. Mensa and K. Vaccaro, "Interpretation of two-dimensional RCS images," in *Proceedings of Antenna Measurement Association Techniques*, September 1988.
- [3] T. H. Lee and W. D. Burnside, "A near field focus procedure using compact range data," in *Proceedings of Antenna Measurement Association Techniques*, September 1988.
- [4] R. J. Marhefka, "Radar cross section - basic scattering code, RCS - BSC (version 2), user's manual," Technical Report 718295, The Ohio State University ElectroScience Laboratory, Department of Electrical Engineering, under preparation 1988. Prepared under Contract No. F33615-86-K-1023 for Wright Patterson Air Force Base.
- [5] W. D. Burnside, J. J. Kim, B. Grandchamp, R. G. Rojas, and P. Law, "Airborne antenna radiation pattern code user's manual," Technical Report 716199-4, The Ohio State University ElectroScience Laboratory, Department of Electrical Engineering, Sep. 1985. Prepared under Grant No. NSG 1498 for National Aeronautics and Space Administration.
- [6] R. J. Marhefka and J. W. Silvestro, "Near zone - basic scattering code, user's manual with space station applications," Technical Report 718422-13, The Ohio State University ElectroScience Laboratory, Department of Electrical Engineering, March 1988. Prepared under Grant No. NSG 1613 for National Aeronautics and Space Administration.

- [7] E. H. Newman and R. L. Dilsavor, "A user's manual for the electromagnetic surface patch code: ESP version III," Technical Report 716148-19, The Ohio State University ElectroScience Laboratory, Department of Electrical Engineering, May 1987. Prepared under Grant No. NSG 1613 for National Aeronautics and Space Administration.